CARPATHIAN J. MATH.
Volume **43** (2027), No. 1,
Pages 139-165

**Online version at https://www.carpathian.cunbm.utcluj.ro/**
**Print Edition: ISSN 1584 - 2851; Online Edition: ISSN 1843 - 4401**
DOI: https://doi.org/10.37193/CJM.2027.01.09

# Multi-view Laplacian twin support vector machine with pinball loss function

VIPAVEE DAMMINSED [1] AND RABIAN WANGKEEREE [2]

ABSTRACT. Multi-view learning is an emerging direction in machine learning that leverages complementary information from multiple distinct feature spaces. In parallel, semi-supervised learning has attracted increasing attention because it can utilize both labeled and unlabeled data to construct more effective classifiers. Motivated by the effectiveness of the Laplacian regularization technique in preserving local manifold structures, we adopt the Laplacian Twin Support Vector Machine (Lap-PTSVM) framework as the foundation of our study. In this work, we extend Lap-PTSVM to the multi-view setting, resulting in the proposed Multi-View Laplacian Twin Support Vector Machine with Pinball Loss Function (MvLapPTSVM) model. We provide a theoretical analysis of its performance and compare it with several state-of-the-art methods. Experimental results demonstrate that the proposed model achieves superior classification performance, confirming its effectiveness and robustness.

## 1. INTRODUCTION

Support Vector Machine (SVM) [1] is an effective and widely used supervised learning model, applicable to both classification and regression tasks. The core idea of SVM is to maximize the margin between two classes by finding the optimal separating hyperplane, formulated as a Quadratic Programming Problem (QPP). SVM has been successfully applied in diverse research areas such as text classification, face recognition, financial analysis, biomedical diagnostics, and human action recognition. Comprehensive discussions of supervised and unsupervised algorithms can be found in [20].

However, one major drawback of SVM is the high computational cost associated with solving a large QPP. To address this limitation, Jayadeva et al. [4] proposed the Twin Support Vector Machine (TSVM), which replaces a single large QPP with two smaller ones. This approach significantly reduces computation time, making TSVM approximately four times faster than the standard SVM. Numerous extensions of TSVM have been developed to improve robustness and generalization, such as the Multi-task Least Squares TSVM [3], Safe Sample Screening for Robust TSVM [8], and Symmetric LINEX Loss TSVM [9]. Several studies have also proposed variants incorporating loss modifications and structural constraints, including the Least Squares Structural Twin Bounded SVM [10] and Intuitionistic Fuzzy TSVM [11]. These works collectively enhance the flexibility and stability of the TSVM framework.

To further improve computational efficiency, Kumar and Gopal (2009) [2] introduced the Least Squares TSVM (LSTSVM), which simplifies training by solving two systems of linear equations instead of QPPs. This formulation inspired additional variants such as the Intuitionistic Fuzzy Weighted LSTSVM (IFW-LSTSVM) [27] and the Robust parametric twin support vector machine [5].

In parallel, several efforts have focused on enhancing the TSVM framework through the introduction of robust and adaptive loss functions. Among these, the Pinball Loss

Received: 03.11.2025. In revised form: 12.02.2026. Accepted: 30.05.2026
2020 *Mathematics Subject Classification.* 68T10, 49N15, 65K10.
Key words and phrases. *Mult-iview Learning,* Twin support vector machine, *Pinball loss function* .
Corresponding author: Rabian Wangkeeree; rabianw@nu.ac.th

function [14] and its extensions have gained increasing attention for their robustness against outliers. Notable developments include the Twin SVM with Pinball Loss [12], the General Twin SVM with Pinball Loss [16], Sparse Pinball TSVM (SPTWSVM) [17], and the Generalized Pinball Loss SVM [18, 19]. These models enhance margin flexibility and improve learning under noise and imbalance conditions.

All of the aforementioned models are based on supervised learning, which requires labeled data for training. In practice, however, most real-world data are unlabeled, and labeling is both time-consuming and costly, particularly in domains requiring expert annotation. To address this challenge, Semi-Supervised Learning (SSL) has been introduced as a hybrid paradigm that leverages both labeled and unlabeled samples to improve learning performance [21]. One of the most successful SSL approaches is the graph-based Laplacian framework, which represents data points as nodes and their pairwise similarities as weighted edges. Based on this concept, several Laplacian-based models have been proposed, such as Laplacian SVM (Lap-SVM), Laplacian TSVM (Lap-TSVM) [22], and Laplacian Least Squares TSVM (Lap-LSTSVM) [23]. More recent extensions, including Laplacian $L_p$-norm LSTSVM [7], demonstrate improved robustness to noise and outliers by employing nonconvex regularization. An extension of Lap-TSVM, known as Lap-PTSVM [24], further improves performance by incorporating the pinball loss, yielding enhanced robustness and efficiency compared to the original Laplacian-based models.

In real-world scenarios, data often contain multiple complementary views that describe the same object or instance. For example, an image can be characterized by various features such as shape, color, and texture, while a video can be represented through both visual and auditory modalities. Multiview learning aims to effectively integrate these diverse feature spaces to achieve better generalization [3]. Due to its ability to exploit complementary information, Multiview Semi-Supervised Learning (MSL) [30] has become an active area of research, combining the strengths of multiview representation and graph-based regularization to learn intrinsic data manifolds from limited labeled data.

However, while models like Lap-PTSVM have been developed for single-view data and demonstrate strong capability in capturing intrinsic data structure through manifold regularization, their extension to multiview scenarios has not been systematically explored. This gap limits their ability to fully leverage inter-view relationships. In this work, we extend the Laplacian Twin Support Vector Machine with Pinball Loss (Lap-PTSVM) to a multiview setting and propose the Multi-View Laplacian Twin Support Vector Machine with Pinball Loss (MvLapPTSVM). The model retains the robustness of the pinball loss while introducing mechanisms for view-specific learning and co-regularization across views. This framework enhances classification accuracy in multiview environments, particularly when labeled data are scarce. The main contributions of this work are as follows.

1. We propose MvLapPTSVM, a novel multi-view extension of Lap-PTSVM with Pinball Loss, combining view-specific learning and co-regularization to handle unlabeled data effectively.

2. We formulate MvLapPTSVM as a Quadratic Programming Problem (QPP), ensuring efficient model training.

3. We validate the proposed method through experiments on benchmark multi-view datasets, showing improved classification performance over existing approaches.

The remainder of this paper is organized as follows. Section 2 presents the preliminaries and notation. The primary and dual formulations of the proposed model are described in Sections 3 and 4, followed by an analysis of its robustness properties. Section 5 discusses the experimental setup and results, and Section 6 concludes the paper.

## 2. PRELIMINARIES

To understand the fundamental concepts, we define the notation and symbols used in this work as follows. For a matrix denoted as $M$ and a vector represented by $x$, their transposes are denoted as $M^\top$ and $x^\top$, respectively. The inverse matrix of $M$ is expressed as $M^{-1}$. Here, we are dealing with a binary semi-supervised classification problem in a $n$-dimensional real space $R^n$. The complete dataset is denoted as $M = (x_1, y_1), \ldots, (x_l, y_l), \ldots, (x_{l+u})$, where $y_i \in \{-1, +1\}$, and $x_i$ for $i = 1, \ldots, l$ represents labeled data, while $x_i$ for $i = l+1, \ldots, l+u$ represents unlabeled data. Assume that we have $l_1$ and $l_2$ samples belonging to the labeled data corresponding to classes +1 and -1, respectively. The positively labeled samples are represented in the matrix $A \in R^{l_1 \times d}$, and the negatively labeled samples are denoted by the matrix $B \in R.^{l_2 \times d}$

2.1. **Twin support vector machine (TSVM).** This method [6] is based on the idea of identifying two nonparallel hyperplanes that classify the data points into their respective classes. It involves a pair of nonparallel planes given by:

$$x^\top w_1 + b_1 = 0 \text{ and } x^\top w_2 + b_2 = 0, \tag{2.1}$$

where $w_1, w_2 \in R^n$ and $b_1, b_2 \in R$. This approach requires solving two small-sized quadratic programming problems (QPPs), formulated as follows:

$$\begin{aligned} \min_{w_1, b_1, \xi} \quad & \frac{1}{2}\|Aw_1 + e_1 b_1\|^2 + c_1 e_2^\top \xi \\ \text{s.t.} \quad & -(Bw_1 + e_2 b_1) + \xi \geq e_2, \\ & \xi \geq 0 \end{aligned} \tag{2.2}$$

and

$$\begin{aligned} \min_{w_2, b_2, \xi} \quad & \frac{1}{2}\|Bw_2 + e_2 b_2\|^2 + c_2 e_1^\top \xi \\ \text{s.t.} \quad & (Aw_2 + e_1 b_2) + \xi \geq e_1, \\ & \xi \geq 0, \end{aligned} \tag{2.3}$$

where $\xi$ are slack variables, $c_1, c_2$ are positive penalty parameters. Although TSVM achieves efficient supervised classification by solving two smaller quadratic problems, it cannot leverage unlabeled data, limiting its use in semi-supervised learning. To address this, Lap-TSVM [22] extends TSVM by incorporating Laplacian regularization through graph-based techniques, allowing the model to utilize both labeled and unlabeled data while preserving the geometric structure of the data distribution.

2.2. **Laplacian Twin support vector machine (Lap-TSVM).** The Lap-TSVM model [22] is formulated by integrating a semi-supervised learning framework derived from the TSVM. As mentioned above, the semi-supervised technique uses the Laplacian matrix, which finds applications in various domains, particularly in spectral graph theory and graph-based machine learning. The Lap-TSVM seeks a pair of nonparallel hyperplanes similar to those in TSVM; however, it differs in that the model learns from both labeled and unlabeled data. The formulation of the problem is as follows.

$$x^\top w_1 + b_1 = 0 \text{ and } x^\top w_2 + b_2 = 0, \tag{2.4}$$

where $w_1, w_2 \in R^n$ and $b_1, b_2 \in R$. The primary problems of this work can be expressed as follows.

$$\begin{aligned} \min_{w_1,b_1,\xi} \quad & \frac{1}{2}\|Aw_1 + e_1b_1\|^2 + c_1e_2^\top\xi + c_2(\|w_1\|^2 + b_1^2) + c_3(w_1^\top M^\top + e^\top b_1)L(Mw_1 + eb_1) \\ \text{s.t.} \quad & -(Bw_1 + e_2b_1) + \xi \geq e_2, \\ & \xi \geq 0, \end{aligned} \tag{2.5}$$

and

$$\begin{aligned} \min_{w_2,b_2,\xi} \quad & \frac{1}{2}\|Bw_2 + e_2b_2\|^2 + c_1e_1^\top\xi + c_2(\|w_2\|^2 + b_2^2) + c_3(w_2^\top M^\top + e^\top b_2)L(Mw_2 + eb_2) \\ \text{s.t.} \quad & Aw_2 + e_1b_2 + \xi \geq e_1, \\ & \xi \geq 0. \end{aligned} \tag{2.6}$$

Here, $M$ is the matrix represents both labeled and unlabeled data. $L$ denotes the graph Laplacian defined as: $L = D - A$, where $D$ is the diagonal matrix of vertex degrees, $A$ is the adjacency matrix of the graph derived from weight matrix defined by k-nearest neighbors, expressed as follows:

$$W_{ij} = \begin{cases} \exp(-\|x_i - x_j\|_2^2/2\sigma^2), & \text{if } x_i, x_j \text{ are neighbor;} \\ 0, & \text{otherwise.} \end{cases} \tag{2.7}$$

The decision function of this problem is derived from

$$\text{class}(i) = \arg\min_{i=1,2} \frac{|x^\top w_i + b_i|}{\|w_i\|}, \tag{2.8}$$

where $|.|$ is the perpendicular distance of point $x$ to the two hyperplanes $x^\top w_1 + b_1$ and $x^\top w_2 + b_2$. In summary, integrating semi-supervised learning into the TSVM framework offers the benefit of utilizing information from both labeled and unlabeled data. This can enhance model performance, particularly in situations where labeled data is limited.

2.3. **Multi-view Laplacian Twin Support Vector Machine (MvLapTSVM).** The MvLapTSVM [31] was developed to efficiently utilize multi-view data from the same source for semi-supervised classification. It adopts the TSVM framework to construct two nonparallel hyperplanes for improved accuracy, while its Laplacian component leverages unlabeled data to capture the intrinsic data structure and enhance generalization when labeled data are limited.

The linear MvLapTSVM is formulated as two optimization problems. In a two-view scenario, the optimization problem for the first class is defined as:

$$\begin{aligned} \min_{w_1,w_2,b_1,b_2,q_1,q_2,\eta} \quad & \frac{1}{2}\left\|A_1'w_1 + e_1b_1\right\|^2 + \frac{1}{2}\left\|A_2'w_2 + e_1b_2\right\|^2 \\ & + c_1e_2^Tq_1 + c_2e_2^Tq_2 + \frac{1}{2}c_3(\|w_1\|^2 + b_1^2 + \|w_2\|^2 + b_2^2) \\ & + \frac{1}{2}c_4[(w_1^TM_1'^T + e^Tb_1)L_1(M_1'w_1 + eb_1) \\ & + (w_2^TM_2'^T + e^Tb_2)L_2(M_2'w_2 + eb_2)] + De_1^T\eta \\ \text{s.t.} \quad & |A_1'w_1 + e_1b_1 - A_2'w_2 - e_1b_2| \leq \eta, \\ & -B_1'w_1 - e_2b_1 + q_1 \geq e_2, \\ & -B_2'w_2 - e_2b_2 + q_2 \geq e_2, \\ & q_1 \geq 0, q_2 \geq 0, \eta \geq 0, \end{aligned} \tag{2.9}$$

and for the second class:

$$
\begin{aligned}
\min_{w_3,w_4,b_3,b_4,q_3,q_4,\zeta} \quad & \frac{1}{2}\left\|B_1' w_3 + e_2 b_3\right\|^2 + \frac{1}{2}\left\|B_2' w_4 + e_2 b_4\right\|^2 \\
& + c_1 e_1^T q_3 + c_2 e_1^T q_4 + \frac{1}{2} c_3 (\|w_3\|^2 + b_3^2 + \|w_4\|^2 + b_4^2) \\
& + \frac{1}{2} c_4 [(w_3^T M_1'^T + e^T b_3) L_1 (M_1' w_3 + e b_3) \\
& + (w_4^T M_2'^T + e^T b_4) L_2 (M_2' w_4 + e b_4)] + H e_2^T \zeta \\
\text{s.t.} \quad & |B_1' w_3 + e_2 b_3 - B_2' w_4 - e_2 b_4| \leq \zeta, \\
& A_1' w_3 + e_1 b_3 + q_3 \geq e_1, \\
& A_2 w_4 + e_1 b_4 + q_4 \geq e_1, \\
& q_3 \geq 0, q_4 \geq 0, \zeta \geq 0,
\end{aligned} \tag{2.10}
$$

where $A_1', B_1'$ and $A_2', B_2'$ are data matrices for the two classes from view 1 and view 2 respectively. $w_i, b_i$ are the weight vectors and biases. $q_i, \eta, \zeta$ are slack variables. $c_i, D, H$ are regularization parameters. $L_1, L_2$ are the graph Laplacians for the two views, and $M_1', M_2'$ include both labeled and unlabeled data.

## 3. Main result

We extend the Lap-PTSVM framework to handle multi-view data by proposing the MvLapPTSVM model. In this work, we divide the data into two views and represent the positive and negative samples from each view separately. Specifically, for view 1, the positive samples are denoted by matrix $A_1'$ and the negative samples by matrix $B_1'$; for view 2, the positive samples are denoted by matrix $A_2'$ and the negative samples by matrix $B_2'$. These matrices are incorporated into the model formulation to enable view-specific learning and co-regularization across views.

3.1. **Primal problem.** In the classification problem, our goal is to define two nonparallel hyperplanes similar to those in (2.9) and (2.10). The problem can be formulated as an optimization problem as follows:

(3.11)

$$
\begin{aligned}
\min_{w_1,b_1,w_2,b_2,q_1,q_2,\eta} \quad & \frac{1}{2}\|A_1^{'} w_1 + e_1 b_1\|^2 + \frac{1}{2}\|A_2^{'} w_2 + e_1 b_2\|^2 + c_1 e_2^{\top} q_1 + c_2 e_2^{\top} q_2 \\
& + \frac{1}{2} c_3 (\|w_1\|^2 + b_1^2 + \|w_2\|^2 + b_2^2) \\
& + \frac{1}{2} c_4 \left[ (M_1^{'} w_1 + e b_1)^{\top} L_1 (M_1^{'} w_1 + e b_1) + (M_2^{'} w_2 + e b_2)^{\top} L_2 (M_2^{'} w_2 + e b_2) \right] \\
& + D e_1^{\top} \eta
\end{aligned}
$$

$$\text{s.t.} \quad |A_1^{'} w_1 + e_1 b_1 - A_2^{'} w_2 - e_1 b_2| \leq \eta, \tag{3.12}$$

$$-(B_1^{'} w_1 + e_2 b_1) + q_1 \geq e_2, \tag{3.13}$$

$$-(B_2^{'} w_2 + e_2 b_2) + q_2 \geq e_2, \tag{3.14}$$

$$-(B_1^{'} w_1 + e_2 b_1) - \frac{q_1}{\tau_1} \leq e_2, \tag{3.15}$$

$$-(B_2^{'} w_2 + e_2 b_2) - \frac{q_2}{\tau_1} \leq e_2, \tag{3.16}$$

$$q_1 \geq 0, q_2 \geq 0, \eta \geq 0, \tag{3.17}$$

and

(3.18)

$$\begin{aligned}\min_{w_3,b_3,w_4,b_4,q_3,q_4,\zeta}\ & \frac{1}{2}\|B_1^{'}w_3+e_2b_3\|^2+\frac{1}{2}\|B_2^{'}w_4+e_2b_4\|^2+c_1e_1^{\top}q_3+c_2e_1^{\top}q_4\\ & +\frac{1}{2}c_3(\|w_3\|^2+b_3^2+\|w_4\|^2+b_4^2)\\ & +\frac{1}{2}c_4\left[(M_1^{'}w_3+eb_3)^{\top}L_1(M_1^{'}w_3+eb_3)+(M_2^{'}w_4+eb_4)^{\top}L_2(M_2^{'}w_4+eb_4)\right]\\ & +He_2^{\top}\zeta\end{aligned}$$

(3.19) s.t. $|B_1^{'}w_3+e_2b_3-B_2^{'}w_4-e_2b_4|\leq\zeta,$

(3.20) $A_1^{'}w_3+e_1b_3+q_3\geq e_1,$

(3.21) $A_2^{'}w_4+e_1b_4+q_4\geq e_1,$

(3.22) $A_1^{'}w_3+e_1b_3-\frac{q_3}{\tau_2}\leq e_1,$

(3.23) $A_2^{'}w_4+e_1b_4-\frac{q_4}{\tau_2}\leq e_1,$

(3.24) $q_3\geq 0, q_4\geq 0, g\geq 0,$

where $e_1$, $e_2$ are vectors with all elements equal to one, used to align with the size of the data.

In problem (3.11), each term in the objective function is designed to balance fitting the labeled data, utilizing unlabeled data, and ensuring robustness across multiple views. The first two terms, $\frac{1}{2}\|A_1'w_1+e_1b_1\|^2$ and $\frac{1}{2}\|A_2'w_2+e_1b_2\|^2$, aim to minimize the sum of the squared distances of positive labeled samples to their respective hyperplanes in each view.

The third term, $c_1e_2^{\top}q_1+c_2e_2^{\top}q_2$, introduces the pinball loss via slack variables $q_1$ and $q_2$, which control the misclassification penalty for negative samples, improving robustness against outliers. The fourth term, $\frac{1}{2}c_3(\|w_1\|^2+b_1^2+\|w_2\|^2+b_2^2)$, serves as a regularization term to prevent overfitting and ill-conditioning by penalizing large weight norms and bias terms. The fifth term, represents the Laplacian regularization. It encourages smoothness in the decision function over the data manifold in each view, leveraging the structure provided by both labeled and unlabeled samples.

The constraints in (3.11) further refine the model behavior. Constraint (3.12) enforces consistency between the decision functions of both views by bounding the difference between their outputs on positive samples within a tolerance $\eta$, acting as a co-regularization mechanism. Constraints (3.13)-(3.16) implement the generalized pinball loss conditions for both views, controlling both lower and upper bounds of slack variables relative to margin violations using parameters $\tau_1$. Finally, constraint (3.17) imposes non-negativity on the slack variables $q_1$, $q_2$, and the tolerance parameter $\eta$, ensuring feasible solutions. The details of the problem in (3.18) follow the same principles as this formulation.

After obtaining the hyperplane for each view, the new view-specific hyperplanes are defined. For new example, two views with feature spaces will be aligned by minimizing the distance between the hyperplanes from both views. This distance is expressed as $\frac{1}{2}\left(\|X_1^{\top}v_1\|+\|X_2^{\top}v_2\|\right)$ or $\frac{1}{2}\left(\|X_1^{\top}u_1\|+\|X_2^{\top}u_2\|\right)$ The process minimizes this alignment distance to make the hyperplanes from both views more consistent, ensuring the model's stability and convergence.

To solve the optimization problems (3.11) and (3.18), we derive their dual formulations and address them through quadratic programming problems (QPPs). Details of this process are presented in the following section.

3.2. **Dual Problem.** Since both optimization problems (3.11) and (3.18) require the same solution process, we present the detailed analysis for (3.11) only. The Lagrangian of the optimization problem (3.11) is defined as follows:

(3.25)

$$\begin{aligned}\mathcal{L} =& \frac{1}{2}\|A_1^{'}w_1 + e_1b_1\|^2 + \frac{1}{2}\|A_2^{'}w_2 + e_1b_2\|^2 + c_1e_2^{\top}q_1 + c_2e_2^{\top}q_2 + \frac{1}{2}c_3(\|w_1\|^2 + b_1^2 + \|w_2\|^2 + b_2^2)\\ &+ \frac{1}{2}c_4\left[(w_1^{\top}M_1^{'\top} + e^{\top}b_1)L_1(M_1^{'}w_1 + eb_1) + (w_2^{\top}M_2^{'\top} + eb_2)L_2(M_2^{'}w_2 + eb_2)\right] + De_1^{\top}\eta\\ &- \beta_1^{\top}(A_1^{'}w_1 + e_1b_1 - A_2^{'}w_2 - e_1b_2 + \eta) - \beta_2^{\top}(\eta - A_1^{'}w_1 - e_1b_1 + A_2^{'}w_2 + e_1b_2)\\ &- \alpha_1^{\top}(-B_1^{'}w_1 - e_2b_1 + q_1 - e_2) - \alpha_2^{\top}(-B_2^{'}w_2 - e_2b_2 + q_2 - e_2)\\ &- \lambda_1^{\top}(e_2 + B_1^{'}w_1 + e_2b_1 + \frac{q_1}{\tau_1}) - \lambda_2^{\top}(e_2 + B_2^{'}w_2 + e_2b_2 + \frac{q_2}{\tau_1})\\ &- \sigma_1^{\top}q_1 - \sigma_2^{\top}q_2 - \gamma^{\top}\eta,\end{aligned}$$

where $\alpha_1, \alpha_2, \beta_1, \beta_2, \lambda_1, \lambda_2, \sigma_1, \sigma_2, \gamma$ are the vectors of nonnegative lagrange multipliers. To derive the optimal conditions, we take the partial derivatives of the above equation with respect to the variables and set them to zero. This yields the following expressions:

$$\begin{aligned}(3.26)\quad \frac{\partial\mathcal{L}}{\partial w_1} &= A_1^{'\top}(A_1^{'}w_1 + e_1b_1) + c_3w_1 + c_4M_1^{'\top}L_1(M_1^{'}w_1 + eb_1) - A_1^{'\top}\beta_1 + A_1^{'\top}\beta_2\\ &\quad + B_1^{'\top}\alpha_1 - B_1^{'\top}\lambda_1 = 0,\\ (3.27)\quad \frac{\partial\mathcal{L}}{\partial b_1} &= e_1^{\top}(A_1^{'}w_1 + e_1b_1) + c_3b_1 + c_4e^{\top}L_1(M_1^{'}w_1 + eb_1) - e_1^{\top}\beta_1 + e_1^{\top}\beta_2\\ &\quad + e_2^{\top}\alpha_1 - e_2^{\top}\lambda_1 = 0,\\ (3.28)\quad \frac{\partial\mathcal{L}}{\partial w_2} &= A_2^{'\top}(A_2^{'}w_2 + e_1b_2) + c_3w_2 + c_4M_2^{'\top}L_2(M_2^{'}w_2 + eb_2) + A_2^{'\top}\beta_1 - A_2^{'\top}\beta_2\\ &\quad + B_2^{'\top}\alpha_2 - B_2^{'\top}\lambda_2 = 0,\\ (3.29)\quad \frac{\partial\mathcal{L}}{\partial b_2} &= e_1^{\top}(A_2^{'}w_2 + e_1b_2) + c_3b_2 + c_4e^{\top}L_2(M_2^{'}w_2 + eb_2) + e_1^{\top}\beta_1 - e_1^{\top}\beta_2\\ &\quad + e_2^{\top}\alpha_2 - e_2^{\top}\lambda_2 = 0,\\ (3.30)\quad \frac{\partial\mathcal{L}}{\partial q_1} &= c_1e_2 - \alpha_1 - \frac{\lambda_1}{\tau_1} - \sigma_1 = 0,\\ (3.31)\quad \frac{\partial\mathcal{L}}{\partial q_2} &= c_2e_2 - \alpha_2 - \frac{\lambda_2}{\tau_1} - \sigma_2 = 0,\\ (3.32)\quad \frac{\partial\mathcal{L}}{\partial \eta} &= De_1 - \beta_1 - \beta_2 - \gamma = 0.\end{aligned}$$

Combine (3.26) and (3.27). Then we get

$$
\begin{aligned}
&A_1^{'\top}(A_1^{'}w_1 + e_1b_1) + e_1^{\top}(A_1^{'}w_1 + e_1b_1) + c_3w_1 + c_3b_1 + c_4M_1^{'\top}L_1(M_1^{'}w_1 + eb_1)\\
&+ c_4e^{\top}L_1(M_1^{'}w_1 + eb_1) - A_1^{'\top}\beta_1 - e_1^{\top}\beta_1 + A_1^{'\top}\beta_2 + e_1^{\top}\beta_2\\
&+ B_1^{'\top}\alpha_1 + e_2^{\top}\alpha_1 - B_1^{'\top}\lambda_1 - e_2^{\top}\lambda_1 = 0,\\
&\begin{bmatrix} A_1^{'\top} \\ e_1^{\top} \end{bmatrix}\begin{bmatrix} A_1^{'} & e_1 \end{bmatrix}\begin{bmatrix} w_1 \\ b_1 \end{bmatrix} + c_3\begin{bmatrix} w_1 \\ b_1 \end{bmatrix} + c_4\begin{bmatrix} M_1^{'\top} \\ e^{\top} \end{bmatrix}L_1\begin{bmatrix} M_1^{'} & e \end{bmatrix}\begin{bmatrix} w_1 \\ b_1 \end{bmatrix}\\
&+ A_1^{'\top}(\beta_2 - \beta_1) + e_1^{\top}(\beta_2 - \beta_1) + B_1^{'\top}(\alpha_1 - \lambda_1) + e_2^{\top}(\alpha_1 - \lambda_1) = 0.
\end{aligned}
$$

Therefore, we obtain

$$
\begin{aligned}
&\begin{bmatrix} A_1^{'\top} \\ e_1^{\top} \end{bmatrix}\begin{bmatrix} A_1^{'} & e_1 \end{bmatrix}\begin{bmatrix} w_1 \\ b_1 \end{bmatrix} + c_3\begin{bmatrix} w_1 \\ b_1 \end{bmatrix} + c_4\begin{bmatrix} M_1^{'\top} \\ e^{\top} \end{bmatrix}L_1\begin{bmatrix} M_1^{'} & e \end{bmatrix}\begin{bmatrix} w_1 \\ b_1 \end{bmatrix}\\
&+ \begin{bmatrix} A_1^{'\top} \\ e_1^{\top} \end{bmatrix}\begin{bmatrix} \beta_2 - \beta_1 \end{bmatrix} + \begin{bmatrix} B_1^{'\top} \\ e_2^{\top} \end{bmatrix}\begin{bmatrix} \alpha_1 - \lambda_1 \end{bmatrix} = 0.
\end{aligned}
$$

Now, we define $A_1 = \begin{bmatrix} A_1^{'} & e_1 \end{bmatrix}$, $A_2 = \begin{bmatrix} A_2^{'} & e_1 \end{bmatrix}$, $B_1 = \begin{bmatrix} B_1^{'} & e_2 \end{bmatrix}$, $B_2 = \begin{bmatrix} B_2^{'} & e_2 \end{bmatrix}$, $J_1 = \begin{bmatrix} M_1^{'} & e \end{bmatrix}$, $J_2 = \begin{bmatrix} M_2^{'} & e \end{bmatrix}$, $v_1 = \begin{bmatrix} w_1 & b_1 \end{bmatrix}^{\top}$, $v_2 = \begin{bmatrix} w_2 & b_2 \end{bmatrix}^{\top}$. Then, we have

$$
\begin{aligned}
A_1^{\top}A_1v_1 + c_3v_1 + c_4J_1^{\top}L_1J_1v_1 + A_1^{\top}(\beta_2 - \beta_1) + B_1^{\top}(\alpha_1 - \lambda_1) &= 0,\\
(A_1^{\top}A_1 + c_3I + c_4J_1^{\top}L_1J_1)v_1 - A_1^{\top}(\beta_1 - \beta_2) - B_1^{\top}(\lambda_1 - \alpha_1) &= 0,\\
(A_1^{\top}A_1 + c_3I + c_4J_1^{\top}L_1J_1)v_1 &= A_1^{\top}(\beta_1 - \beta_2) + B_1^{\top}(\lambda_1 - \alpha_1).
\end{aligned}
$$

Now, we obtain

$$v_1 = (A_1^{\top}A_1 + c_3I + c_4J_1^{\top}L_1J_1)^{-1}[A_1^{\top}(\beta_1 - \beta_2) + \beta_1^{\top}(\lambda_1 - \alpha_1)].$$

Similarly, we apply the same process to (3.28) and (3.29) as follows:

$$
\begin{aligned}
&A_2^{'\top}(A_2^{'}w_2 + e_1b_2) + e_1^{\top}(A_2^{'}w_2 + e_1b_2) + c_3w_2 + c_3b_2 + c_4M_2^{'\top}L_2(M_2^{'}w_2 + eb_2)\\
&+ c_4e^{\top}L_2(M_2^{'}w_2 + eb_2) + A_2^{'\top}\beta_1 + e_1^{\top}\beta_1 - A_2^{'\top}\beta_2 + -e_1^{\top}\beta_2\\
&+ B_2^{'\top}\alpha_2 + e_2^{\top}\alpha_2 - B_2^{'\top}\lambda_2 - e_2^{\top}\lambda_2 = 0,\\
&\begin{bmatrix} A_2^{'\top} \\ e_1^{\top} \end{bmatrix}\begin{bmatrix} A_2^{'} & e_1 \end{bmatrix}\begin{bmatrix} w_2 \\ b_2 \end{bmatrix} + c_3\begin{bmatrix} w_2 \\ b_2 \end{bmatrix} + c_4\begin{bmatrix} M_2^{'\top} \\ e^{\top} \end{bmatrix}L_2\begin{bmatrix} M_2^{'} & e \end{bmatrix}\begin{bmatrix} w_2 \\ b_2 \end{bmatrix}\\
&+ A_2^{'\top}(\beta_1 - \beta_2) + e_1^{\top}(\beta_1 - \beta_2) + B_2^{'\top}(\alpha_2 - \lambda_2) + e_2^{\top}(\alpha_2 - \lambda_2) = 0.
\end{aligned}
$$

Therefore, we obtain

$$
\begin{aligned}
&\begin{bmatrix} A_2^{'\top} \\ e_1^{\top} \end{bmatrix}\begin{bmatrix} A_2^{'} & e_1 \end{bmatrix}\begin{bmatrix} w_2 \\ b_2 \end{bmatrix} + c_3\begin{bmatrix} w_2 \\ b_2 \end{bmatrix} + c_4\begin{bmatrix} M_2^{'\top} \\ e^{\top} \end{bmatrix}L_2\begin{bmatrix} M_2^{'} & e \end{bmatrix}\begin{bmatrix} w_2 \\ b_2 \end{bmatrix}\\
&+ \begin{bmatrix} A_2^{'\top} \\ e_1^{\top} \end{bmatrix}\begin{bmatrix} \beta_1 - \beta_2 \end{bmatrix} + \begin{bmatrix} B_2^{'\top} \\ e_2^{\top} \end{bmatrix}\begin{bmatrix} \alpha_2 - \lambda_2 \end{bmatrix} = 0.
\end{aligned}
$$

Then, we have

$$\begin{aligned} A_2^\top A_2 v_2 + c_3 v_2 + c_4 J_2^\top L_2 J_2 v_2 + A_2^\top(\beta_1 - \beta_2) + B_2^\top(\alpha_2 - \lambda_2) &= 0, \\ (A_2^\top A_2 + c_3 I + c_4 J_2^\top L_2 J_2) v_2 - A_2^\top(\beta_2 - \beta_1) - B_2^\top(\lambda_2 - \alpha_2) &= 0, \\ (A_2^\top A_2 + c_3 I + c_4 J_2^\top L_2 J_2) v_2 &= A_2^\top(\beta_2 - \beta_1) + B_1^\top(\lambda_2 - \alpha_2). \end{aligned}$$

Now, we get

$$v_2 = (A_2^\top A_2 + c_3 I + c_4 J_2^\top L_2 J_2)^{-1}[A_2^\top(\beta_2 - \beta_1) + B_2^\top(\lambda_2 - \alpha_2)].$$

From the above equations, we obtain the solution forms for $w$ and $b$ as follows:

$$v_1 = (A_1^\top A_1 + c_3 I + c_4 J_1^\top L_1 J_1)^{-1}[A_1^\top(\beta_1 - \beta_2) + B_1^\top(\lambda_1 - \alpha_1)], \tag{3.33}$$

$$v_2 = (A_2^\top A_2 + c_3 I + c_4 J_2^\top L_2 J_2)^{-1}[A_2^\top(\beta_2 - \beta_1) + B_2^\top(\lambda_2 - \alpha_2)]. \tag{3.34}$$

Similarly, for the problem (3.18), we obtain:

$$v_3 = (B_1^\top B_1 + c_3 I + c_4 J_1^\top L_1 J_1)^{-1}[B_1^\top(\beta_3 - \beta_4) - A_1^\top(\lambda_3 - \alpha_3)], \tag{3.35}$$

$$v_4 = (B_2^\top B_2 + c_3 I + c_4 J_2^\top L_2 J_2)^{-1}[B_2^\top(\beta_4 - \beta_3) - A_2^\top(\lambda_4 - \alpha_4)], \tag{3.36}$$

where $v_3 = \begin{bmatrix} w_3 & b_3 \end{bmatrix}^\top$ and $v_4 = \begin{bmatrix} w_4 & b_4 \end{bmatrix}^\top$. We substitute (3.33) and (3.34) into (3.25) and get the dual form problem of (3.11) as

(3.37)

$$\begin{aligned} \min_{\xi_1,\xi_2,\alpha_1,\alpha_2} \quad & \frac{1}{2}\xi_1^\top (A_1^\top A_1 + c_3 I + c_4 J_1^\top L_1 J_1)^{-1}\xi_1 + \frac{1}{2}\xi_2^\top (A_2^\top A_2 + c_3 I + c_4 J_2^\top L_2 J_2)^{-1}\xi_2 \\ & + (\lambda_1 - \alpha_1 + \lambda_2 - \alpha_2)^\top e_2 \\ \text{s.t.} \quad & \xi_1 = (A_1^\top(\beta_1 - \beta_2) + B_1^\top(\lambda_1 - \alpha_1)), \\ & \xi_2 = (A_2^\top(\beta_2 - \beta_1) + B_1^\top(\lambda_2 - \alpha_2)), \\ & \lambda_1, \lambda_2, \alpha_1, \alpha_2, \beta_1, \beta_2 \geq 0, \\ & c_1 e_2 \geq \frac{\lambda_1}{\tau_1} + \alpha_1, \\ & c_2 e_2 \geq \frac{\lambda_2}{\tau_1} + \alpha_2, \\ & \beta_1 + \beta_2 \leq D e_1, \end{aligned}$$

and also the same process, we substitute (3.35) and (3.36) into (3.18), then we obtain dual problem as follow:

(3.38)

$$\begin{aligned}\min_{\xi_3,\xi_4,\alpha_3,\alpha_4}\ & \frac{1}{2}\xi_3^\top(B_1^\top B_1+c_3I+c_4J_1^\top L_1J_1)^{-1}\xi_3+\frac{1}{2}\xi_4^\top(B_2^\top B_2+c_3I+c_4J_2^\top L_2J_2)^{-1}\xi_4\\ &+(\lambda_3-\alpha_3+\lambda_4-\alpha_4)^\top e_1\\ \text{s.t. }\ & \xi_3=(B_1^\top(\beta_3-\beta_4)-A_1^\top(\lambda_3-\alpha_3)),\\ & \xi_4=(B_2^\top(\beta_4-\beta_3)-A_2^\top(\lambda_4-\alpha_4)),\\ & \lambda_3,\lambda_4,\alpha_3,\alpha_4,\beta_3,\beta_4\geq 0,\\ & c_1e_1\geq\frac{\lambda_3}{\tau_2}+\alpha_3,\\ & c_2e_1\geq\frac{\lambda_4}{\tau_2}+\alpha_4,\\ & \beta_3+\beta_4\leq He_2,\end{aligned}$$

where $\xi_3,\xi_4\geq 0$. By solving the QPPs, we obtain the optimal solution and subsequently determine $w_1,w_2,w_3,w_4$ and $b_1,b_2,b_3,b_4$. After obtaining the hyperplanes for each view, the new view-specific hyperplanes are defined. For the new example, in the case of two views with feature spaces $x_1$ and $x_2$, alignment is achieved by minimizing the distance between the hyperplanes from both views. This distance is expressed as $\frac{1}{2}\left(\|X_1^\top v_1\|+\|X_2^\top v_2\|\right)$ and $\frac{1}{2}\left(\|X_1^\top v_3\|+\|X_2^\top v_4\|\right)$.

To establish the theoretical properties of the proposed MvLapPTSVM model, we analyze the dual problem (3.37). Since the dual problem (3.38) has an analogous structure, the same analysis can be applied similarly. Therefore, in the following results, we focus only on the theoretical analysis of (3.37).

**Lemma 3.1.** *Let*

$$G_i=A_i^\top A_i+c_3I+c_4J_i^\top L_iJ_i,\qquad i=1,2,$$

*where $L_i$ is the graph Laplacian matrix constructed from a symmetric nonnegative weight matrix $W_i$. Then*

$$G_i\succ 0,\qquad i=1,2.$$

*Proof.* Let $u$ be any nonzero vector in $R^n$. It is enough to show that

$$u^\top G_iu>0.$$

By the definition of $G_i$,

$$u^\top G_iu=u^\top A_i^\top A_iu+c_3u^\top u+c_4u^\top J_i^\top L_iJ_iu.$$

We first verify that $L_i\succeq 0$. For any $z=(z_1,\ldots,z_n)^\top$,

$$z^\top L_iz=z^\top(D_i-W_i)z=z^\top D_iz-z^\top W_iz.$$

Since $(D_i)_{jj}=\sum_k(W_i)_{jk}$, we have

$$z^\top D_iz=\sum_j(D_i)_{jj}z_j^2=\sum_{j,k}(W_i)_{jk}z_j^2,$$

and

$$z^\top W_iz=\sum_{j,k}(W_i)_{jk}z_jz_k.$$

Hence,

$$z^\top L_i z = \sum_{j,k} (W_i)_{jk} z_j^2 - \sum_{j,k} (W_i)_{jk} z_j z_k.$$

Using the symmetry $(W_i)_{jk} = (W_i)_{kj}$, we obtain

$$\sum_{j,k} (W_i)_{jk} z_j^2 = \frac{1}{2} \sum_{j,k} (W_i)_{jk} (z_j^2 + z_k^2).$$

Therefore,

$$\begin{aligned} z^\top L_i z &= \frac{1}{2} \sum_{j,k} (W_i)_{jk} (z_j^2 + z_k^2) - \sum_{j,k} (W_i)_{jk} z_j z_k \\ &= \frac{1}{2} \sum_{j,k} (W_i)_{jk} (z_j - z_k)^2 \geq 0. \end{aligned}$$

Thus,

$$L_i \succeq 0.$$

Now,

$$u^\top A_i^\top A_i u = \|A_i u\|^2 \geq 0, \qquad u^\top u = \|u\|^2 > 0.$$

Since $L_i \succeq 0$, taking $z = J_i u$ gives

$$u^\top J_i^\top L_i J_i u = (J_i u)^\top L_i (J_i u) \geq 0.$$

Consequently,

$$u^\top G_i u = \|A_i u\|^2 + c_3 \|u\|^2 + c_4 (J_i u)^\top L_i (J_i u) > 0.$$

Hence,

$$G_i \succ 0.$$

This completes the proof. □

**Theorem 3.1.** *The dual problem* (3.37) *is a convex quadratic programming problem with a convex feasible region.*

*Proof.* By the previous lemma, we obtain $G_i^{-1} \succ 0,\ i = 1, 2$. Since $\xi_i$ is linear in the dual variables, the quadratic terms

$$\frac{1}{2} \xi_i^\top G_i^{-1} \xi_i, \qquad i = 1, 2,$$

are convex quadratic functions.
Moreover,

$$(\lambda_1 - \alpha_1 + \lambda_2 - \alpha_2)^\top e_2$$

is linear. Therefore, the objective function in (3.37) is convex quadratic.

Furthermore, all constraints in (3.37) are affine equality and affine inequality constraints. Hence, the feasible region is convex. Consequently, the dual problem (3.37) is a convex quadratic programming problem. □

**Remark 3.1.** *The same result also holds for the dual problem* (3.38)*, since it has an analogous structure.*

**Theorem 3.2.** *The dual problem* (3.37) *admits at least one optimal solution.*

*Proof.* By the previous lemma, we have $G_i^{-1}$ exists for $i = 1, 2$.
Moreover, by the previous theorem, the optimization problem (3.37) is a convex quadratic programming problem. Now consider the feasible set of (3.37):

$$\mathcal{D} = \Big\{(\alpha, \lambda, \beta) \;\Big|\; \alpha_i \geq 0,\ \lambda_i \geq 0,\ \beta_i \geq 0, \quad i = 1, 2,$$
$$\alpha_i + \frac{\lambda_i}{\tau_1} \leq c_i e_2, \quad i = 1, 2,$$
$$\beta_1 + \beta_2 \leq De_1\Big\}.$$

Clearly, $\alpha_1 = \alpha_2 = \lambda_1 = \lambda_2 = \beta_1 = \beta_2 = 0$ satisfies all constraints. Hence, $\mathcal{D} \neq \emptyset$.
Next, the inequalities

$$\alpha_i + \frac{\lambda_i}{\tau_1} \leq c_i e_2$$

together with

$$\alpha_i \geq 0, \qquad \lambda_i \geq 0$$

imply that $\alpha_i$ and $\lambda_i$ are bounded componentwise.
Similarly,

$$0 \leq \beta_1, \beta_2, \qquad \beta_1 + \beta_2 \leq De_1$$

implies that $\beta_1$ and $\beta_2$ are bounded componentwise.
Therefore, $\mathcal{D}$ is closed and bounded. Hence, $\mathcal{D}$ is compact. The dual objective function corresponding to (3.37) is continuous on $\mathcal{D}$. Therefore, by the Weierstrass theorem, there exists

$$(\alpha^*, \lambda^*, \beta^*) \in \mathcal{D}$$

such that the dual objective function attains its optimal value.
Hence, the dual problem (3.37) admits at least one optimal solution. □

**Remark 3.2.** *The same existence result also holds for the dual problem* (3.38)*, since it has an analogous feasible set and objective structure.*

**Corollary 3.1.** *The optimization problem* (3.37) *admits a unique optimal solution.*

*Proof.* By the previous lemma, we have $G_i^{-1} \succ 0,\ i = 1, 2$. Hence, the objective function in (3.37) is strictly convex. Since the feasible region is convex by the previous theorem, the optimization problem (3.37) admits a unique minimizer. □

**Remark 3.3.** *The same uniqueness result also holds for the dual problem* (3.38)*.*

**Corollary 3.2.** *Let* $(\alpha_1^*, \alpha_2^*, \lambda_1^*, \lambda_2^*, \beta_1^*, \beta_2^*)$ *be an optimal solution of the dual problem* (3.37)*. Then the corresponding primal solution*

$$v_1^* = \begin{bmatrix} w_1^* \\ b_1^* \end{bmatrix}, \qquad v_2^* = \begin{bmatrix} w_2^* \\ b_2^* \end{bmatrix}$$

*is obtained by*

$$v_1^* = G_1^{-1}\left[A_1^\top(\beta_1^* - \beta_2^*) + B_1^\top(\lambda_1^* - \alpha_1^*)\right],$$

*and*

$$v_2^* = G_2^{-1}\left[A_2^\top(\beta_2^* - \beta_1^*) + B_2^\top(\lambda_2^* - \alpha_2^*)\right].$$

*Proof.* From the optimal solution of primal problem (3.11), we have (3.33) and (3.34) as follow:

$$\begin{aligned} v_1 &= (A_1^\top A_1 + c_3 I + c_4 J_1^\top L_1 J_1)^{-1}[A_1^\top(\beta_1 - \beta_2) + B_1^\top(\lambda_1 - \alpha_1)], \\ v_2 &= (A_2^\top A_2 + c_3 I + c_4 J_2^\top L_2 J_2)^{-1}[A_2^\top(\beta_2 - \beta_1) + B_2^\top(\lambda_2 - \alpha_2)]. \end{aligned}$$

Therefore,

$$v_1 = G_1^{-1}\left[A_1^\top(\beta_1 - \beta_2) + B_1^\top(\lambda_1 - \alpha_1)\right],$$

and

$$v_2 = G_2^{-1}\left[A_2^\top(\beta_2 - \beta_1) + B_2^\top(\lambda_2 - \alpha_2)\right].$$

Substituting the optimal dual solution $(\alpha^*, \lambda^*, \beta^*)$ into the above expressions gives the desired result. □

**Remark 3.4.** *The same reconstruction and decision mechanism also hold for the dual problem* (3.38).

The resulting view-specific hyperplanes are defined by

$$(x^{(1)})^\top w_1^* + b_1^* = 0, \qquad (x^{(2)})^\top w_2^* + b_2^* = 0,$$

for the positive class, and

$$(x^{(1)})^\top w_3^* + b_3^* = 0, \qquad (x^{(2)})^\top w_4^* + b_4^* = 0,$$

for the negative class, where $x^{(1)}$ and $x^{(2)}$ denote the feature representations of a sample from the first and second views, respectively.

To enhance the consistency between multiple views, the proposed MvLapPTSVM model minimizes the average fitting distance between the view-specific hyperplanes. Let $X_1$ and $X_2$ denote the data matrices corresponding to the first and second views, respectively. Accordingly, the multiview distances for the positive and negative classes are defined by

$$d_+(x) = \frac{1}{2}\left(\|X_1^\top v_1^*\| + \|X_2^\top v_2^*\|\right),$$

and

$$d_-(x) = \frac{1}{2}\left(\|X_1^\top v_3^*\| + \|X_2^\top v_4^*\|\right),$$

respectively.

Therefore, the final decision function is given by

$$\hat{y}(x) = \begin{cases} +1, & d_+(x) \le d_-(x), \\ -1, & d_+(x) > d_-(x), \end{cases}$$

where $\hat{y}(x)$ denotes the predicted class label of the sample $x$.

## 4. Numerical examples

In this experiment, we evaluated six TSVM-based models, TSVM, TPSVM, MvTSVM [31], MvTPMSVM [26], Lap-PTSVM, and MvLapPTSVM. The models were tested across 10 benchmark [29] datasets including Australian, Bupa, Spectfheart, Phoneme, Monk-2, Ring, Ionsphere, WBDC, Diabetes and Sonar. The detial of dataset is shown in Table 1.

To ensure fairness, a 5-fold cross-validation procedure was employed. For each dataset and each model, we report the fold-wise accuracy and F1-score, along with their corresponding averages and standard deviations. The computation time was also recorded. All experiments were conducted in Python on a machine equipped with an Intel® Core™ i7-8700 CPU @ 3.20,GHz and 16,GB of RAM.

For multiview-based models (MvTSVM, MvTPMSVM, and MvLapPTSVM), each dataset was represented using two feature views. The first view corresponds to the original feature representation of the dataset. The second view was constructed by applying Principal Component Analysis (PCA) is applied to the original features in order to obtain an alternative lower-dimensional embedding of the same samples. PCA was fitted separately

within each fold to avoid information leakage, and the resulting projected features were used as the second view for all multiview models.

TABLE 1. Dataset information.

| Dataset | Dimensions (samples × features) |
|---|---|
| Australian | 690 × 14 |
| Bupa | 345 × 6 |
| Diabetes | 768 × 8 |
| Inosphere | 351 × 33 |
| Monk-2 | 432 × 6 |
| Phoneme | 5404 × 5 |
| Ring | 7400 × 20 |
| Sonar | 208 × 60 |
| Spectfheart | 267 × 44 |
| WDBC | 569 × 30 |

For the experiments, we set the proportion of labeled data to 30% and 50% to evaluate the benefits of incorporating the Laplacian term within the multi-view framework. All results, including fold-wise accuracy, computation time, and F1-score, are reported, with the highest accuracy values highlighted in bold. The results are illustrated in Tables 2 and 3.

TABLE 2. The results of five-fold cross-validation on 30% labeled data, including Accuracy and F1-score for each fold, comparing the models with our proposed method.

| **Model** | Acc(%)<br>F1<br>**fold-1** | Acc(%)<br>F1<br>**fold-2** | Acc(%)<br>F1<br>**fold-3** | Acc(%)<br>F1<br>**fold-4** | Acc(%)<br>F1<br>**fold-5** | Avg Acc<br>Avg F1 | **Average**<br>Time(s) |
|---|---|---|---|---|---|---|---|
| **Australian** | | | | | | | |
| MvLapPTSVM | 72.46 | 77.54 | 76.09 | 68.84 | 72.46 | $73.48 \pm 3.06$ | 0.0988 |
| | 71.60 | 76.77 | 75.80 | 68.71 | 72.18 | $73.01 \pm 2.94$ | |
| LapPTSVM | 89.86 | 85.51 | 82.61 | 83.33 | 86.23 | $\mathbf{85.51 \pm 2.55}$ | 0.1129 |
| | 89.80 | 85.48 | 82.59 | 83.33 | 86.23 | $85.49 \pm 2.54$ | |
| MvTPMSVM | 88.41 | 84.78 | 84.06 | 85.51 | 83.33 | $85.22 \pm 1.75$ | 0.0576 |
| | 88.16 | 84.74 | 84.00 | 85.36 | 83.26 | $85.10 \pm 1.68$ | |
| MvTSVM | 89.86 | 83.33 | 83.33 | 84.06 | 83.33 | $84.78 \pm 2.55$ | 0.0340 |
| | 89.78 | 83.31 | 83.29 | 83.94 | 83.33 | $84.73 \pm 2.54$ | |
| TPSVM | 89.13 | 84.78 | 83.33 | 82.61 | 84.78 | $84.93 \pm 2.26$ | 0.0275 |
| | 89.06 | 84.74 | 83.18 | 83.61 | 84.78 | $84.87 \pm 2.26$ | |
| TSVM | 90.58 | 85.51 | 82.61 | 83.33 | 86.23 | $85.65 \pm 2.80$ | 0.0143 |
| | 90.54 | 85.48 | 82.59 | 83.33 | 86.23 | $85.64 \pm 2.79$ | |
| **Bupa** | | | | | | | |
| MvLapPTSVM | 71.01 | 78.26 | 65.22 | 66.67 | 62.32 | $\mathbf{68.70 \pm 5.55}$ | 0.0712 |
| | 68.06 | 75.80 | 60.87 | 60.10 | 58.47 | $64.66 \pm 6.47$ | |
| LapPTSVM | 63.77 | 68.12 | 57.97 | 60.87 | 66.67 | $63.48 \pm 3.71$ | 0.0710 |
| | 56.63 | 61.28 | 42.25 | 43.83 | 57.53 | $52.30 \pm 7.74$ | |

TABLE 2. (continued) The results of five-fold cross-validation on 30% labeled data, including Accuracy and F1-score for each fold, comparing the models with our proposed method.

| **Model** | Acc(%)<br>F1<br>**fold-1** | Acc(%)<br>F1<br>**fold-2** | Acc(%)<br>F1<br>**fold-3** | Acc(%)<br>F1<br>**fold-4** | Acc(%)<br>F1<br>**fold-5** | Avg Acc<br>Avg F1 | **Average**<br>Time(s) |
|---|---|---|---|---|---|---|---|
| MvTPMSVM | 69.57 | 69.57 | 68.12 | 68.12 | 68.12 | $68.70 \pm 0.71$ | 0.0313 |
| | 66.77 | 68.26 | 63.30 | 64.86 | 66.94 | $66.03 \pm 1.74$ | |
| MvTSVM | 69.57 | 69.57 | 68.12 | 68.12 | 68.12 | $68.70 \pm 0.71$ | 0.0182 |
| | 66.77 | 68.26 | 63.30 | 64.86 | 66.94 | $66.03 \pm 1.74$ | |
| TPSVM | 62.32 | 66.67 | 59.42 | 68.12 | 68.12 | $64.93 \pm 3.48$ | 0.0119 |
| | 56.62 | 65.24 | 57.41 | 66.53 | 67.95 | $62.75 \pm 4.77$ | |
| TSVM | 62.32 | 66.67 | 59.42 | 68.12 | 68.12 | $64.93 \pm 3.48$ | 0.0085 |
| | 56.62 | 65.24 | 57.41 | 66.53 | 67.95 | $62.75 \pm 4.77$ | |
| **Diabetes** | | | | | | | |
| MvLapPTSVM | 77.27 | 74.68 | 83.12 | 73.20 | 72.55 | $\mathbf{76.16 \pm 3.84}$ | 0.0926 |
| | 74.22 | 71.82 | 79.85 | 69.06 | 67.75 | $72.54 \pm 4.29$ | |
| LapPTSVM | 75.32 | 75.97 | 79.87 | 72.55 | 73.86 | $75.51 \pm 2.48$ | 0.1031 |
| | 70.17 | 71.50 | 73.61 | 64.46 | 67.65 | $69.48 \pm 3.17$ | |
| MvTPMSVM | 76.62 | 75.97 | 80.52 | 75.16 | 71.24 | $75.90 \pm 2.97$ | 0.0543 |
| | 73.06 | 73.27 | 76.14 | 71.16 | 66.22 | $71.97 \pm 3.29$ | |
| MvTSVM | 77.27 | 74.68 | 82.47 | 73.86 | 71.90 | $76.03 \pm 3.65$ | 0.0283 |
| | 73.95 | 72.07 | 78.94 | 70.29 | 67.18 | $72.49 \pm 3.92$ | |
| TPSVM | 75.97 | 75.97 | 80.52 | 73.86 | 72.55 | $75.77 \pm 2.71$ | 0.0261 |
| | 72.16 | 73.73 | 75.80 | 70.29 | 67.75 | $71.95 \pm 2.77$ | |
| TSVM | 75.97 | 75.97 | 80.52 | 73.86 | 72.55 | $75.77 \pm 2.71$ | 0.0184 |
| | 72.16 | 73.73 | 75.80 | 70.29 | 67.75 | $71.95 \pm 2.77$ | |
| **Ionosphere** | | | | | | | |
| MvLapPTSVM | 83.10 | 87.14 | 77.14 | 90.00 | 90.00 | $\mathbf{85.48 \pm 4.87}$ | 0.0966 |
| | 80.24 | 84.48 | 74.64 | 88.25 | 88.79 | $83.28 \pm 5.30$ | |
| LapPTSVM | 88.73 | 87.14 | 75.71 | 84.29 | 82.86 | $83.75 \pm 4.52$ | 0.3459 |
| | 87.41 | 84.48 | 67.62 | 80.45 | 78.33 | $79.66 \pm 6.79$ | |
| MvTPMSVM | 70.42 | 87.14 | 78.57 | 85.71 | 88.57 | $82.08 \pm 6.77$ | 0.0422 |
| | 60.19 | 84.90 | 74.83 | 82.99 | 86.39 | $77.86 \pm 9.70$ | |
| MvTSVM | 70.42 | 88.57 | 74.29 | 90.00 | 90.00 | $82.66 \pm 8.52$ | 0.0497 |
| | 60.19 | 86.39 | 68.50 | 88.25 | 88.54 | $78.37 \pm 11.78$ | |
| TPSVM | 66.20 | 82.86 | 71.43 | 88.57 | 88.57 | $79.53 \pm 9.14$ | 0.0182 |
| | 46.62 | 79.59 | 63.88 | 86.74 | 87.05 | $72.78 \pm 15.55$ | |
| TSVM | 66.20 | 82.86 | 71.43 | 88.57 | 87.14 | $79.24 \pm 8.87$ | 0.0164 |
| | 46.62 | 79.59 | 63.88 | 86.74 | 85.26 | $72.42 \pm 15.23$ | |
| **Monk-2** | | | | | | | |
| MvLapPTSVM | 72.41 | 82.76 | 84.88 | 86.05 | 81.40 | $81.50 \pm 4.82$ | 0.0741 |
| | 72.12 | 82.76 | 84.88 | 85.98 | 81.40 | $81.43 \pm 4.92$ | |
| LapPTSVM | 80.46 | 82.76 | 82.56 | 81.40 | 81.40 | $\mathbf{81.71 \pm 0.85}$ | 0.0853 |
| | 80.20 | 82.72 | 82.44 | 81.40 | 81.30 | $81.61 \pm 0.90$ | |
| MvTPMSVM | 73.56 | 77.01 | 88.37 | 82.56 | 77.91 | $79.88 \pm 5.12$ | 0.0307 |

TABLE 2. (continued) The results of five-fold cross-validation on 30% labeled data, including Accuracy and F1-score for each fold, comparing the models with our proposed method.

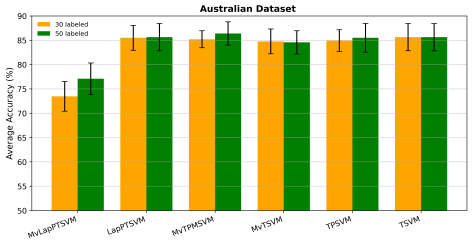
| **Model** | Acc(%) F1 **fold-1** | Acc(%) F1 **fold-2** | Acc(%) F1 **fold-3** | Acc(%) F1 **fold-4** | Acc(%) F1 **fold-5** | Avg Acc Avg F1 | **Average** Time(s) |
|---|---|---|---|---|---|---|---|
| | 73.56 | 76.98 | 88.37 | 82.56 | 77.90 | $79.87 \pm 5.13$ | |
| MvTSVM | 71.26 | 72.41 | 81.40 | 86.05 | 69.77 | $76.18 \pm 6.39$ | 0.0249 |
| | 71.13 | 72.23 | 81.30 | 86.04 | 69.75 | $76.09 \pm 6.42$ | |
| TPSVM | 79.31 | 78.16 | 80.23 | 83.72 | 86.05 | $81.49 \pm 2.94$ | 0.0195 |
| | 77.76 | 77.87 | 79.77 | 83.71 | 85.86 | $80.99 \pm 3.25$ | |
| TSVM | 65.52 | 66.67 | 75.58 | 75.58 | 72.09 | $71.09 \pm 4.29$ | 0.0104 |
| | 58.86 | 63.40 | 73.33 | 74.82 | 69.74 | $68.03 \pm 6.04$ | |
| **Phoneme** | | | | | | | |
| MvLapPTSVM | 75.39 | 75.67 | 76.13 | 74.38 | 71.57 | $74.63 \pm 1.63$ | 0.8759 |
| | 71.14 | 71.86 | 72.83 | 70.76 | 69.38 | $71.19 \pm 1.15$ | |
| LapPTSVM | 72.25 | 73.91 | 72.43 | 70.49 | 70.74 | $71.96 \pm 1.25$ | 4.6123 |
| | 53.07 | 58.18 | 55.15 | 54.87 | 50.56 | $54.37 \pm 2.51$ | |
| MvTPMSVM | 70.68 | 70.68 | 70.68 | 70.58 | 70.65 | $70.65 \pm 0.04$ | 0.6138 |
| | 41.41 | 41.41 | 41.41 | 41.38 | 41.40 | $41.40 \pm 0.01$ | |
| MvTSVM | 74.28 | 76.23 | 76.41 | 74.47 | 73.98 | $\mathbf{75.07 \pm 1.03}$ | 0.0880 |
| | 66.27 | 68.00 | 68.64 | 68.61 | 65.18 | $67.34 \pm 1.38$ | |
| TPSVM | 72.25 | 74.65 | 72.90 | 73.27 | 71.20 | $72.85 \pm 1.14$ | 0.1955 |
| | 62.70 | 65.40 | 63.52 | 65.84 | 62.11 | $63.91 \pm 1.47$ | |
| TSVM | 68.46 | 70.31 | 71.69 | 68.64 | 67.78 | $69.37 \pm 1.43$ | 0.0257 |
| | 67.49 | 68.77 | 70.39 | 67.73 | 66.86 | $68.25 \pm 1.23$ | |
| **Ring** | | | | | | | |
| MvLapPTSVM | 72.70 | 74.32 | 63.24 | 75.27 | 64.39 | $69.99 \pm 5.12$ | 1.6878 |
| | 70.57 | 73.08 | 60.99 | 75.23 | 62.47 | $68.47 \pm 5.72$ | |
| LapPTSVM | 76.28 | 74.53 | 76.49 | 76.55 | 77.43 | $\mathbf{76.26 \pm 0.95}$ | 7.2903 |
| | 76.04 | 74.27 | 76.27 | 76.30 | 77.17 | $76.01 \pm 0.95$ | |
| MvTPMSVM | 49.53 | 49.53 | 49.53 | 49.53 | 49.46 | $49.51 \pm 0.03$ | 1.0368 |
| | 33.12 | 33.12 | 33.12 | 33.12 | 33.09 | $33.12 \pm 0.01$ | |
| MvTSVM | 76.22 | 74.26 | 77.30 | 74.66 | 76.49 | $75.78 \pm 1.15$ | 0.2529 |
| | 75.92 | 73.96 | 77.08 | 74.34 | 76.19 | $75.50 \pm 1.17$ | |
| TPSVM | 73.78 | 72.16 | 73.78 | 72.36 | 74.66 | $73.35 \pm 0.95$ | 0.4573 |
| | 73.77 | 72.10 | 73.71 | 72.29 | 74.66 | $73.31 \pm 0.97$ | |
| TSVM | 71.08 | 70.47 | 71.42 | 69.53 | 68.99 | $70.30 \pm 0.92$ | 0.0571 |
| | 68.31 | 67.60 | 68.90 | 66.38 | 65.62 | $67.36 \pm 1.21$ | |
| **Sonar** | | | | | | | |
| MvLapPTSVM | 69.05 | 57.14 | 71.43 | 82.93 | 78.05 | $\mathbf{71.72 \pm 8.79}$ | 0.0869 |
| | 69.03 | 57.14 | 71.43 | 81.85 | 75.99 | $71.09 \pm 8.23$ | |
| LapPTSVM | 61.90 | 66.67 | 73.81 | 75.61 | 78.05 | $71.21 \pm 6.00$ | 0.3239 |
| | 61.82 | 66.67 | 73.79 | 73.72 | 76.66 | $70.53 \pm 5.46$ | |
| MvTPMSVM | 64.29 | 57.14 | 71.43 | 60.98 | 73.17 | $65.40 \pm 6.09$ | 0.0469 |
| | 64.10 | 57.05 | 71.17 | 59.80 | 72.58 | $64.94 \pm 6.11$ | |

TABLE 2. (continued) The results of five-fold cross-validation on 30% labeled data, including Accuracy and F1-score for each fold, comparing the models with our proposed method.

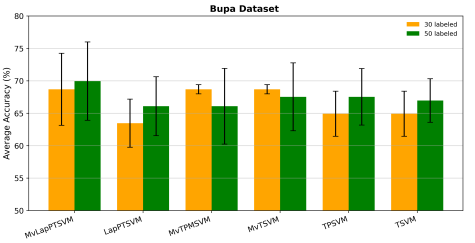
| **Model** | Acc(%)<br>F1<br>**fold-1** | Acc(%)<br>F1<br>**fold-2** | Acc(%)<br>F1<br>**fold-3** | Acc(%)<br>F1<br>**fold-4** | Acc(%)<br>F1<br>**fold-5** | Avg Acc<br>Avg F1 | **Average**<br>Time(s) |
|---|---|---|---|---|---|---|---|
| MvTSVM | 61.90 | 54.76 | 69.05 | 65.85 | 70.73 | $64.46 \pm 5.71$ | 0.0632 |
| | 61.82 | 54.74 | 69.03 | 65.67 | 68.46 | $63.94 \pm 5.26$ | |
| TPSVM | 66.67 | 57.14 | 59.52 | 87.80 | 63.41 | $66.91 \pm 10.94$ | 0.0203 |
| | 66.67 | 57.05 | 59.50 | 87.80 | 62.61 | $66.73 \pm 11.02$ | |
| TSVM | 64.29 | 57.14 | 59.52 | 87.80 | 60.98 | $65.95 \pm 11.17$ | 0.0269 |
| | 64.27 | 57.05 | 59.50 | 87.80 | 59.80 | $65.68 \pm 11.30$ | |
| **Spectfheart** | | | | | | | |
| MvLapPTSVM | 77.78 | 81.48 | 73.58 | 71.70 | 69.81 | $74.87 \pm 4.23$ | 0.0984 |
| | 55.98 | 58.97 | 62.30 | 41.76 | 41.11 | $52.02 \pm 8.88$ | |
| LapPTSVM | 61.11 | 53.70 | 52.83 | 67.92 | 64.15 | $59.94 \pm 5.87$ | 0.3865 |
| | 52.49 | 41.07 | 46.68 | 52.80 | 54.90 | $49.59 \pm 5.06$ | |
| MvTPMSVM | 81.48 | 79.63 | 81.13 | 75.47 | 75.47 | $78.64 \pm 2.66$ | 0.0959 |
| | 58.97 | 51.90 | 53.01 | 43.01 | 43.01 | $49.98 \pm 6.18$ | |
| MvTSVM | 83.33 | 79.63 | 81.13 | 75.47 | 75.47 | $\mathbf{79.01 \pm 3.12}$ | 0.0999 |
| | 65.16 | 51.90 | 53.01 | 43.01 | 43.01 | $51.22 \pm 8.16$ | |
| TPSVM | 70.37 | 62.96 | 73.58 | 73.58 | 67.92 | $69.69 \pm 3.98$ | 0.0707 |
| | 59.47 | 49.34 | 64.33 | 62.30 | 55.51 | $58.19 \pm 5.32$ | |
| TSVM | 70.37 | 55.56 | 71.71 | 71.70 | 67.92 | $67.45 \pm 6.10$ | 0.0944 |
| | 59.47 | 44.62 | 62.73 | 60.74 | 55.51 | $56.61 \pm 6.45$ | |
| **WBDC** | | | | | | | |
| MvLapPTSVM | 94.74 | 90.35 | 95.61 | 92.98 | 94.69 | $93.67 \pm 1.87$ | 0.1095 |
| | 94.35 | 89.94 | 95.31 | 92.53 | 94.32 | $93.29 \pm 1.90$ | |
| LapPTSVM | 93.86 | 97.37 | 92.98 | 95.61 | 96.46 | $95.26 \pm 1.62$ | 0.3789 |
| | 93.37 | 97.21 | 92.11 | 95.26 | 96.21 | $94.83 \pm 1.86$ | |
| MvTPMSVM | 92.98 | 96.46 | 94.74 | 96.49 | 99.12 | $\mathbf{95.96 \pm 2.04}$ | 0.0655 |
| | 92.53 | 96.27 | 94.15 | 96.15 | 99.05 | $95.63 \pm 2.20$ | |
| MvTSVM | 94.74 | 96.49 | 96.49 | 97.37 | 94.69 | $95.96 \pm 1.06$ | 0.0497 |
| | 94.40 | 96.33 | 96.15 | 97.13 | 94.42 | $95.68 \pm 1.09$ | |
| TPSVM | 94.74 | 96.49 | 92.11 | 95.61 | 93.81 | $94.55 \pm 1.51$ | 0.0266 |
| | 94.22 | 96.30 | 91.28 | 95.16 | 93.34 | $94.06 \pm 1.70$ | |
| TSVM | 93.86 | 92.98 | 92.11 | 93.86 | 91.15 | $92.79 \pm 1.05$ | 0.0236 |
| | 93.49 | 92.71 | 91.38 | 93.22 | 90.69 | $92.30 \pm 1.08$ | |

As shown in Table 2, across the ten benchmark datasets, the empirical results indicate that all six TSVM-based methods achieve competitive performance under the 30% labeled data. In most datasets, the multiview variants yield higher or comparable accuracy and F1-scores compared to the standard TSVM baseline, suggesting that incorporating alternative feature views can be beneficial when labeled data are limited.

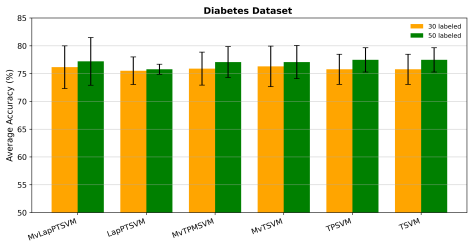
For instance, on the *Australian*, MvLapPTSVM achieved 73.48% accuracy and 73.01% F1, which is noticeably inferior to the TSVM baseline (85.65% accuracy and 85.64% F1). In



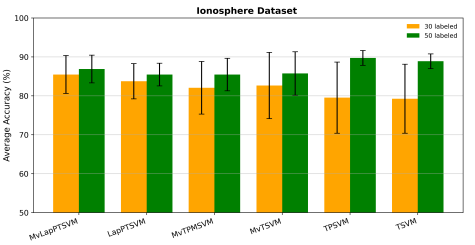

(A) Australian



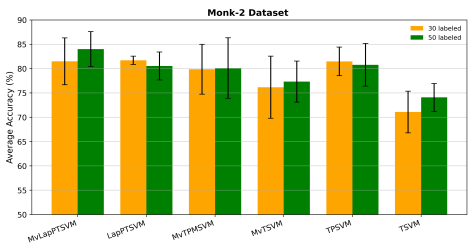

(B) Bupa



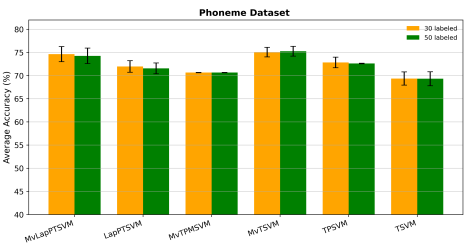

(C) Diabetes



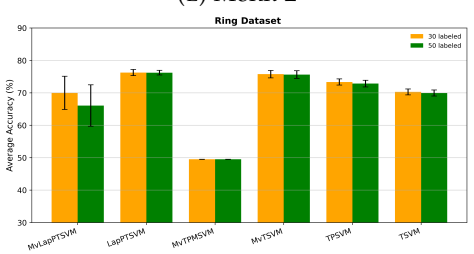

(D) Ionosphere



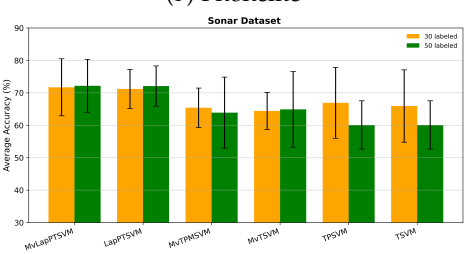

(E) Monk-2



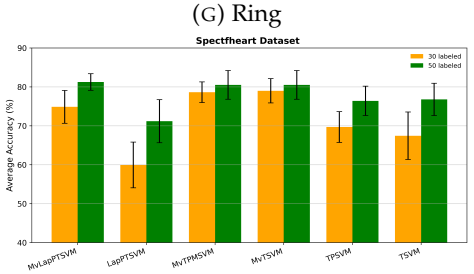

(F) Phoneme



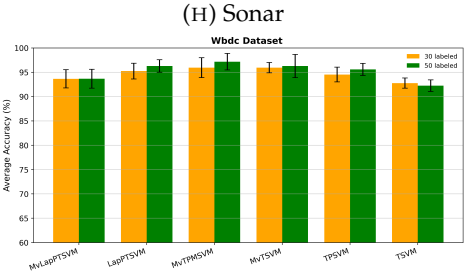

(G) Ring




(H) Sonar




(I) Spectfheart




(J) Wbdc

FIGURE 1. Comparison of average classification accuracy for 30% and 50% labeled data.

contrast, on the *Ionosphere*, the proposed attained 85.48% accuracy and 83.28% F1, outperforming the TSVM baseline (79.24% accuracy and 72.42% F1). Similarly, on the *Phoneme* and *Sonar*, our model remains competitive or superior to TSVM in both metrics, illustrating that its relative advantage is dataset-dependent.

Compared with other multiview extensions, our proposed model remains within a similar performance range rather than clearly dominating them, while incurring higher computation time due to the Laplacian regularization. Nevertheless, it consistently outperforms its single-view counterpart, Lap-PTSVM, demonstrating the effectiveness of integrating multi-view information for improved classification under limited labeled data. Overall, the proposed approach can be regarded as a competitive and robust option in low-label scenarios.

TABLE 3. The results of five-fold cross-validation on 50% labeled data, including Accuracy and F1-score for each fold, comparing the models with our proposed method.

| **Model** | Acc(%)<br>F1<br>**fold-1** | Acc(%)<br>F1<br>**fold-2** | Acc(%)<br>F1<br>**fold-3** | Acc(%)<br>F1<br>**fold-4** | Acc(%)<br>F1<br>**fold-5** | Avg Acc<br>Avg F1 | **Average**<br>Time(s) |
|---|---|---|---|---|---|---|---|
| **Australian** | | | | | | | |
| MvLapPTSVM | 73.19 | 78.99 | 80.43 | 73.19 | 79.71 | $77.10 \pm 3.23$ | 0.1218 |
| | 72.67 | 78.49 | 79.40 | 73.02 | 79.50 | $76.61 \pm 3.10$ | |
| LapPTSVM | 90.58 | 85.51 | 82.61 | 83.33 | 86.23 | $\mathbf{85.65 \pm 2.80}$ | 0.1485 |
| | 90.54 | 85.48 | 82.59 | 83.33 | 86.23 | $85.64 \pm 2.79$ | |
| MvTPMSVM | 89.13 | 81.88 | 84.06 | 84.06 | 84.06 | $84.64 \pm 2.40$ | 0.0813 |
| | 89.06 | 81.84 | 84.03 | 83.94 | 84.05 | $84.58 \pm 2.39$ | |
| MvTSVM | 89.86 | 81.88 | 83.33 | 84.06 | 84.78 | $84.78 \pm 2.71$ | 0.0428 |
| | 89.90 | 81.88 | 83.31 | 83.97 | 84.78 | $84.75 \pm 2.70$ | |
| TPSVM | 90.58 | 85.51 | 81.88 | 83.33 | 86.23 | $85.51 \pm 2.97$ | 0.0320 |
| | 90.54 | 85.48 | 81.86 | 83.33 | 86.23 | $85.49 \pm 2.96$ | |
| TSVM | 90.58 | 85.51 | 82.61 | 83.33 | 86.23 | $\mathbf{85.65 \pm 2.80}$ | 0.0159 |
| | 90.54 | 85.48 | 82.59 | 83.33 | 86.23 | $85.64 \pm 2.79$ | |
| **Bupa** | | | | | | | |
| MvLapPTSVM | 68.12 | 75.36 | 68.12 | 66.67 | 56.52 | $66.96 \pm 6.04$ | 0.0869 |
| | 64.13 | 73.10 | 64.86 | 62.08 | 47.19 | $62.27 \pm 8.42$ | |
| LapPTSVM | 73.91 | 63.77 | 68.12 | 63.77 | 60.87 | $66.09 \pm 4.55$ | 0.0949 |
| | 68.32 | 52.15 | 61.28 | 57.77 | 50.15 | $57.93 \pm 6.53$ | |
| MvTPMSVM | 66.67 | 73.91 | 63.77 | 69.57 | 56.52 | $66.09 \pm 5.84$ | 0.0362 |
| | 61.15 | 71.77 | 61.12 | 68.26 | 47.19 | $61.90 \pm 8.43$ | |
| MvTSVM | 71.01 | 73.91 | 63.77 | 69.57 | 59.42 | $\mathbf{67.54 \pm 5.23}$ | 0.0245 |
| | 66.63 | 71.77 | 61.12 | 68.26 | 50.71 | $63.70 \pm 7.35$ | |
| TPSVM | 75.36 | 68.12 | 66.67 | 65.22 | 62.32 | $67.54 \pm 4.36$ | 0.0173 |
| | 71.97 | 64.86 | 65.24 | 64.31 | 57.61 | $64.80 \pm 4.55$ | |
| TSVM | 72.46 | 68.12 | 66.67 | 65.22 | 62.32 | $66.96 \pm 3.36$ | 0.0133 |
| | 69.35 | 64.86 | 65.24 | 64.31 | 57.61 | $64.27 \pm 3.78$ | |
| **Diabetes** | | | | | | | |
| MvLapPTSVM | 75.32 | 79.22 | 84.42 | 75.16 | 71.90 | $77.20 \pm 4.29$ | 0.1020 |

TABLE 3. (continued) The results of five-fold cross-validation on 50% labeled data, including Accuracy and F1-score for each fold, comparing the models with our proposed method.

| **Model** | Acc(%)<br>F1<br>**fold-1** | Acc(%)<br>F1<br>**fold-2** | Acc(%)<br>F1<br>**fold-3** | Acc(%)<br>F1<br>**fold-4** | Acc(%)<br>F1<br>**fold-5** | Avg Acc<br>Avg F1 | **Average**<br>Time(s) |
|---|---|---|---|---|---|---|---|
| | 71.87 | 76.77 | 81.40 | 71.16 | 66.37 | 73.51 ± 5.14 | |
| LapPTSVM | 75.97 | 75.32 | 77.27 | 74.51 | 75.82 | 75.78 ± 0.90 | 0.1462 |
| | 70.36 | 69.35 | 69.70 | 67.26 | 70.29 | 69.39 ± 1.13 | |
| MvTPMSVM | 77.27 | 77.92 | 81.17 | 76.47 | 72.55 | 77.08 ± 2.77 | 0.0738 |
| | 73.66 | 74.56 | 77.38 | 72.36 | 67.75 | 73.14 ± 3.16 | |
| MvTSVM | 76.62 | 77.92 | 81.82 | 76.47 | 72.55 | 77.08 ± 2.98 | 0.0401 |
| | 73.06 | 74.83 | 78.02 | 72.68 | 67.75 | 73.27 ± 3.34 | |
| TPSVM | 77.27 | 78.57 | 80.52 | 77.12 | 73.86 | **77.47 ± 2.18** | 0.0385 |
| | 73.95 | 76.16 | 75.80 | 73.59 | 68.92 | 73.68 ± 2.59 | |
| TSVM | 77.277 | 78.57 | 80.52 | 77.12 | 73.86 | **77.47 ± 2.18** | 0.0132 |
| | 73.95 | 76.16 | 75.80 | 73.59 | 68.92 | 73.68 ± 2.59 | |
| **Ionosphere** | | | | | | | |
| MvLapPTSVM | 87.32 | 88.57 | 80.00 | 88.57 | 90.00 | 86.89 ± 3.55 | 0.0968 |
| | 85.69 | 86.39 | 74.72 | 86.39 | 88.25 | 84.29 ± 4.86 | |
| LapPTSVM | 85.92 | 88.57 | 81.43 | 82.86 | 88.57 | 85.47 ± 2.92 | 0.0979 |
| | 84.26 | 86.39 | 76.90 | 79.59 | 86.39 | 82.71 ± 3.82 | |
| MvTPMSVM | 85.92 | 91.43 | 78.57 | 84.29 | 87.14 | 85.47 ± 4.18 | 0.0611 |
| | 85.06 | 90.49 | 74.13 | 81.99 | 85.59 | 83.45 ± 5.44 | |
| MvTSVM | 87.32 | 92.86 | 75.71 | 85.71 | 87.14 | 85.75 ± 5.58 | 0.0486 |
| | 86.45 | 91.81 | 68.77 | 83.81 | 84.90 | 83.15 ± 7.70 | |
| TPSVM | 90.14 | 90.00 | 87.14 | 88.57 | 92.86 | **89.74 ± 1.90** | 0.0281 |
| | 89.29 | 88.54 | 85.59 | 87.05 | 91.81 | 88.46 ± 2.11 | |
| TSVM | 88.73 | 90.00 | 85.71 | 88.57 | 91.43 | 88.89 ± 1.89 | 0.0199 |
| | 87.65 | 88.54 | 84.15 | 87.05 | 90.29 | 87.53 ± 2.01 | |
| **Monk-2** | | | | | | | |
| MvLapPTSVM | 79.31 | 88.51 | 86.05 | 86.05 | 80.23 | **84.03 ± 3.60** | 0.0733 |
| | 79.24 | 88.47 | 86.04 | 85.98 | 80.23 | 83.99 ± 3.60 | |
| LapPTSVM | 77.01 | 85.06 | 81.40 | 81.40 | 77.91 | 80.55 ± 2.87 | 0.1033 |
| | 76.94 | 85.06 | 81.30 | 81.39 | 77.88 | 80.51 ± 2.89 | |
| MvTPMSVM | 72.41 | 75.86 | 89.53 | 84.88 | 77.91 | 80.12 ± 6.22 | 0.0457 |
| | 72.38 | 75.81 | 89.53 | 84.83 | 77.90 | 80.09 ± 6.23 | |
| MvTSVM | 72.41 | 74.71 | 81.40 | 84.88 | 73.26 | 77.33 ± 4.22 | 0.0245 |
| | 72.32 | 74.63 | 81.30 | 84.88 | 73.22 | 77.27 ± 4.94 | |
| TPSVM | 87.36 | 73.56 | 80.23 | 81.40 | 81.40 | 80.79 ± 4.39 | 0.0256 |
| | 86.91 | 73.21 | 79.77 | 81.39 | 81.23 | 80.50 ± 4.39 | |
| TSVM | 70.11 | 72.41 | 73.26 | 77.91 | 76.74 | 74.09 ± 2.86 | 0.0127 |
| | 65.77 | 70.71 | 70.33 | 77.39 | 75.41 | 71.92 ± 4.10 | |
| **Phoneme** | | | | | | | |
| MvLapPTSVM | 76.04 | 74.65 | 75.86 | 71.69 | 73.06 | 74.26 ± 1.67 | 0.9395 |

TABLE 3. (continued) The results of five-fold cross-validation on 50% labeled data, including Accuracy and F1-score for each fold, comparing the models with our proposed method.

| **Model** | Acc(%)<br>F1<br>**fold-1** | Acc(%)<br>F1<br>**fold-2** | Acc(%)<br>F1<br>**fold-3** | Acc(%)<br>F1<br>**fold-4** | Acc(%)<br>F1<br>**fold-5** | Avg Acc<br>Avg F1 | **Average**<br>Time(s) |
|---|---|---|---|---|---|---|---|
| | 72.41 | 71.06 | 70.05 | 68.56 | 70.52 | 70.52 ± 1.26 | |
| LapPTSVM | 71.97 | 72.62 | 72.80 | 69.75 | 70.65 | 71.56 ± 1.18 | 16.8690 |
| | 56.55 | 53.70 | 56.40 | 55.06 | 51.09 | 54.56 ± 2.02 | |
| MvTPMSVM | 70.68 | 70.68 | 70.68 | 70.58 | 70.65 | 70.65 ± 0.04 | 0.9234 |
| | 41.41 | 41.41 | 41.41 | 41.38 | 41.40 | 41.40 ± 0.01 | |
| MvTSVM | 74.93 | 76.50 | 76.50 | 74.10 | 74.26 | **75.26 ± 1.05** | 0.1665 |
| | 67.83 | 68.73 | 68.81 | 67.90 | 66.25 | 67.90 ± 0.92 | |
| TPSVM | 72.80 | 73.54 | 72.90 | 71.42 | 72.41 | 72.61 ± 0.70 | 0.3607 |
| | 63.89 | 64.79 | 63.79 | 63.56 | 64.00 | 64.01 ± 0.42 | |
| TSVM | 68.18 | 70.40 | 71.79 | 68.36 | 67.877 | 69.32 ± 1.52 | 0.0355 |
| | 67.26 | 69.03 | 70.50 | 67.53 | 66.98 | 68.26 ± 1.32 | |
| **Ring** | | | | | | | |
| MvLapPTSVM | 68.18 | 55.95 | 63.65 | 75.54 | 67.16 | 66.09 ± 6.38 | 1.9263 |
| | 67.22 | 44.76 | 61.52 | 75.48 | 66.05 | 63.01 ± 10.18 | |
| LapPTSVM | 76.08 | 75.41 | 76.62 | 75.61 | 77.43 | **76.23 ± 0.73** | 26.1214 |
| | 75.79 | 75.12 | 76.40 | 75.34 | 77.14 | 75.96 ± 0.74 | |
| MvTPMSVM | 49.53 | 49.53 | 49.53 | 49.53 | 49.46 | 49.51 ± 0.03 | 1.9764 |
| | 33.12 | 33.12 | 33.12 | 33.12 | 33.09 | 33.12 ± 0.01 | |
| MvTSVM | 76.08 | 74.26 | 77.23 | 74.32 | 76.35 | 75.65 ± 1.17 | 0.4022 |
| | 75.78 | 73.91 | 77.00 | 74.02 | 76.05 | 75.35 ± 0.12 | |
| TPSVM | 73.24 | 71.42 | 72.77 | 72.36 | 74.53 | 72.86 ± 1.03 | 0.8744 |
| | 73.21 | 71.34 | 72.73 | 72.79 | 74.52 | 72.82 ± 1.05 | |
| TSVM | 70.81 | 70.00 | 71.08 | 68.58 | 69.26 | 69.95 ± 0.94 | 0.1019 |
| | 67.98 | 67.00 | 68.39 | 65.07 | 66.05 | 66.90 ± 1.22 | |
| **Sonar** | | | | | | | |
| MvLapPTSVM | 71.43 | 57.14 | 73.81 | 78.05 | 80.49 | **72.18 ± 8.16** | 0.1065 |
| | 71.36 | 57.14 | 73.79 | 77.84 | 79.90 | 72.01 ± 8.01 | |
| LapPTSVM | 80.95 | 64.29 | 73.81 | 65.85 | 75.61 | 72.10 ± 6.22 | 0.0645 |
| | 80.78 | 64.27 | 73.68 | 65.34 | 74.88 | 71.79 ± 6.20 | |
| MvTPMSVM | 83.33 | 64.29 | 50.00 | 58.54 | 63.41 | 63.91 ± 10.95 | 0.0786 |
| | 83.32 | 64.27 | 49.28 | 55.91 | 63.33 | 63.32 ± 11.43 | |
| MvTSVM | 85.71 | 61.90 | 50.00 | 60.98 | 65.85 | 64.89 ± 11.67 | 0.0829 |
| | 85.68 | 61.82 | 48.57 | 59.00 | 65.67 | 64.15± 12.17 | |
| TPSVM | 73.81 | 52.38 | 54.76 | 60.98 | 58.4 | 60.09 ± 7.47 | 0.0331 |
| | 73.68 | 52.38 | 54.11 | 59.00 | 58.44 | 59.52 ± 7.51 | |
| TSVM | 73.81 | 52.38 | 54.76 | 60.98 | 58.54 | 60.09 ± 7.47 | 0.0231 |
| | 73.68 | 52.38 | 54.11 | 59.00 | 58.44 | 59.52± 7.51 | |
| **Spectfheart** | | | | | | | |
| MvLapPTSVM | 83.33 | 81.48 | 77.36 | 83.02 | 81.13 | **81.26 ± 2.13** | 0.1073 |

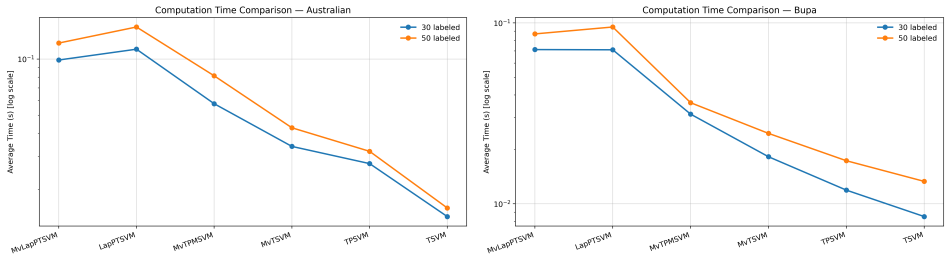
TABLE 3. (continued) The results of five-fold cross-validation on 50% labeled data, including Accuracy and F1-score for each fold, comparing the models with our proposed method.

| **Model** | Acc(%) F1 **fold-1** | Acc(%) F1 **fold-2** | Acc(%) F1 **fold-3** | Acc(%) F1 **fold-4** | Acc(%) F1 **fold-5** | Avg Acc Avg F1 | **Average** Time(s) |
|---|---|---|---|---|---|---|---|
| | 68.58 | 58.97 | 63.02 | 71.14 | 63.19 | $64.98 \pm 4.34$ | |
| LapPTSVM | 68.52 | 62.96 | 77.36 | 69.81 | 77.36 | $71.20 \pm 5.53$ | 0.0680 |
| | 45.71 | 38.64 | 69.42 | 54.11 | 59.85 | $53.55 \pm 10.73$ | |
| MvTPMSVM | 81.48 | 79.63 | 86.79 | 79.25 | 75.47 | $80.52 \pm 3.69$ | 0.0614 |
| | 53.13 | 51.90 | 77.56 | 61.47 | 43.01 | $57.41 \pm 11.65$ | |
| MvTSVM | 81.48 | 79.63 | 86.79 | 79.25 | 75.47 | $80.52 \pm 3.69$ | 0.0592 |
| | 53.13 | 51.90 | 77.56 | 61.47 | 43.01 | $57.41 \pm 11.65$ | |
| TPSVM | 79.63 | 70.37 | 79.25 | 79.25 | 73.58 | $76.42 \pm 3.77$ | 0.0381 |
| | 51.90 | 41.30 | 64.73 | 57.29 | 42.39 | $51.52 \pm 8.90$ | |
| TSVM | 81.48 | 70.37 | 79.25 | 79.25 | 73.58 | $76.79 \pm 4.14$ | 0.0331 |
| | 58.97 | 41.30 | 64.73 | 57.29 | 42.39 | $52.94 \pm 9.39$ | |
| **WBDC** | | | | | | | |
| MvLapPTSVM | 95.61 | 90.35 | 93.86 | 92.98 | 95.58 | $93.68 \pm 1.95$ | 0.1407 |
| | 95.31 | 89.68 | 93.37 | 92.53 | 95.24 | $93.23 \pm 2.07$ | |
| LapPTSVM | 94.74 | 98.25 | 95.61 | 95.61 | 97.35 | $96.31 \pm 1.29$ | 0.1286 |
| | 94.40 | 98.13 | 95.16 | 95.13 | 97.14 | $96.03 \pm 1.39$ | |
| MvTPMSVM | 94.74 | 98.25 | 95.61 | 99.12 | 98.23 | $\mathbf{97.19 \pm 1.70}$ | 0.0885 |
| | 94.29 | 98.12 | 95.16 | 99.05 | 98.09 | $96.94 \pm 1.86$ | |
| MvTSVM | 92.98 | 98.25 | 93.86 | 98.25 | 98.23 | $96.31 \pm 2.38$ | 0.0681 |
| | 92.60 | 98.15 | 93.22 | 98.12 | 98.11 | $96.04 \pm 2.56$ | |
| TPSVM | 93.86 | 97.37 | 94.74 | 96.49 | 95.58 | $95.61 \pm 1.24$ | 0.0368 |
| | 93.30 | 97.24 | 94.15 | 96.15 | 95.19 | $95.21 \pm 1.40$ | |
| TSVM | 95.61 | 95.61 | 96.49 | 92.98 | 95.58 | $92.26 \pm 1.19$ | 0.0249 |
| | 95.35 | 95.39 | 96.19 | 92.53 | 95.33 | $94.96 \pm 1.26$ | |

As shown in Table 3, which presents the experiments conducted under the 50% labeled data, all models generally exhibited performance improvements across most datasets, reflecting the benefit of increased supervision. Among them, our proposed model demonstrated consistently competitive results, achieving top or near-top accuracy in several datasets such as *Spectfheart*, *Monk-2*, and *Ring*. The incorporation of Laplacian regularization within the multiview learning framework enhanced representation consistency between views, contributing to stable performance gains. However, this improvement was accompanied by a moderate increase in computational time compared to the simpler TSVM and MvTSVM models, which is an expected trade-off resulting from the additional graph-based regularization structure.

Compared to the 30% labeled-data scenario, the performance of MvLapPTSVM remained stable or even slightly improved, indicating that the model is robust across different levels of label density. Although the relative ranking among the models remained

largely consistent, the accuracy gap between the Laplacian-based and non-Laplacian variants gradually narrowed as more labeled data were provided, suggesting that the regularization effect is more beneficial under low-label conditions. Nevertheless, the proposed model continued to generalize well while preserving its multiview advantage. Increasing the proportion of labeled data did not cause overfitting or noticeably increase computation time. All comparative average accuracy results for the 30% and 50% labeled data are presented in Figure 1. As shown in Figure 2, the Laplacian-based multiview mod-




(A) Computation time for the *Australian*. (B) Computation time for the *Bupa*.

FIGURE 2. Average computation time comparison for the dataset under 30% and 50% labeled data (log scale).

els (LapPTSVM and MvLapTSVM) consistently require longer computation times than TSVM and TPSVM. This is an expected effect of the additional graph-regularization terms used to stabilize the decision boundary under limited supervision. Therefore, the increase in runtime reflects a methodological trade-off rather than computational inefficiency.

TABLE 4. Model ranking performance based on 30% labeled data across all datasets.

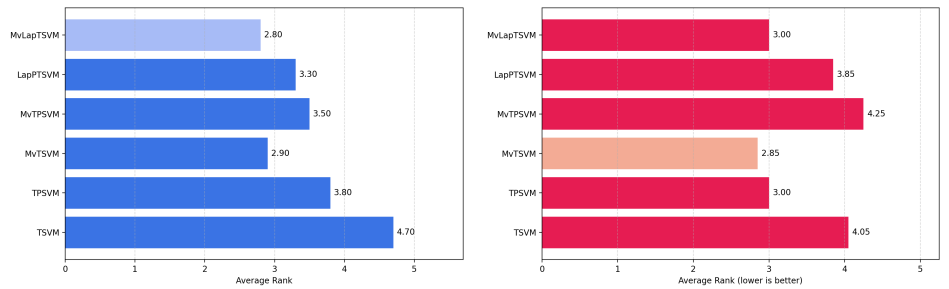
| **Dataset** | **MvLapPTSVM** | **Lap-PTSVM** | **MvTPSVM** | **MvTSVM** | **TPSVM** | **TSVM** |
|---|---|---|---|---|---|---|
| Australian | 6 | 2 | 3 | 5 | 4 | 1 |
| Bupa | 2 | 6 | 2 | 2 | 4.5 | 4.5 |
| Diabetes | 1 | 6 | 3 | 2 | 4.5 | 4.5 |
| Ionosphere | 1 | 2 | 4 | 5 | 3 | 6 |
| Monk-2 | 2 | 4 | 5 | 1 | 3 | 6 |
| Phoneme | 5 | 1 | 6 | 2 | 3 | 4 |
| Ring | 3 | 6 | 2 | 1 | 4 | 5 |
| Sonar | 3 | 6 | 2 | 1 | 4 | 5 |
| Spectfheart | 3 | 6 | 2 | 1 | 4 | 5 |
| WBDC | 5 | 3 | 1 | 2 | 4 | 6 |
| **Sum** | **28** | **33** | **35** | **29** | **38** | **47** |
| **Average Rank** | **2.8** | **3.3** | **3.5** | **2.9** | **3.8** | **4.7** |

In addition, we ranked all models based on their classification accuracy across datasets, assigning rank 1 to the model with the highest accuracy and increasing ranks (2, 3, ..., 6) to those with lower performance. A lower average rank therefore indicates better overall performance. Across the ten benchmark datasets, the average ranks in Tables 4 and 5 show a consistent trend between the 30% and 50% labeled. Under the 30% setting, MvLapPTSVM achieves the best average rank (2.8), followed closely by MvTSVM (2.9),

TABLE 5. Model ranking performance based on 50% labeled data across all datasets.

| Dataset | MvLapPTSVM | Lap-PTSVM | MvTPSVM | MvTSVM | TPSVM | TSVM |
|---|---|---|---|---|---|---|
| Australian | 6 | 1.5 | 5 | 4 | 3 | 1.5 |
| Bupa | 3 | 6 | 5 | 1 | 2 | 4 |
| Diabetes | 3 | 6 | 5 | 4 | 1.5 | 1.5 |
| Ionosphere | 3 | 6 | 5 | 4 | 1 | 2 |
| Monk-2 | 1 | 3 | 4 | 5 | 2 | 6 |
| Phoneme | 2 | 4 | 5 | 1 | 3 | 6 |
| Ring | 5 | 1 | 6 | 2 | 3 | 4 |
| Sonar | 1 | 6 | 2.5 | 2.5 | 5 | 4 |
| Spectfheart | 5 | 3 | 4 | 1 | 2 | 6 |
| WBDC | 1 | 3 | 4 | 2 | 5.5 | 5.5 |
| **Sum** | **30** | **38.5** | **42.5** | **28.5** | **30** | **40.5** |
| **Average Rank** | **3.0** | **3.85** | **4.25** | **2.85** | **3.0** | **4.05** |

whereas TSVM records the worst average rank (4.7). A similar pattern is observed under the 50% labeled condition, where MvLapPTSVM and MvTSVM again obtain the lowest average ranks (3.0 and 2.85, respectively), while TSVM remains the highest-ranked model (4.05). Although no single method dominates all datasets individually, the multi-view approaches consistently achieve lower average ranks than the single-view methods in both labeling regimes. This consistency in rank distributions suggests that increasing the labeled proportion does not substantially alter the relative competitiveness among the methods. The ranking results are also illustrated in Figure 3, where a lower value indicates better performance.




(A) 30% labeled data (B) 50% labeled data

FIGURE 3. Average rank comparison of classification accuracy for all models across benchmark datasets.

4.1. **Statistical Analysis.** To statistically compare the performance of the six classification models across multiple datasets, the nonparametric Friedman test [13], [15] was employed. This test evaluates whether significant differences exist among the average ranks of the algorithms across $N$ datasets. Let $r_{ij}$ denote the rank of the $j$-th algorithm on the $i$-th dataset, where the best-performing algorithm on each dataset receives rank 1. The

average rank of algorithm $j$ is given by

$$R_j = \frac{1}{N}\sum_{i=1}^{N} r_{ij}. \tag{4.39}$$

The Friedman statistic is then computed as

$$\chi_F^2 = \frac{12N}{k(k+1)}\left(\sum_{j=1}^{k} R_j^2 - \frac{k(k+1)^2}{4}\right), \tag{4.40}$$

$$F_F = \frac{(N-1)\,\chi_F^2}{N(k-1)-\chi_F^2}, \tag{4.41}$$

where $k$ is the number of algorithms. This statistic is approximately $\chi^2$-distributed with $k-1$ degrees of freedom.

**Case 1: 30% labeled data.** For the 30% labeled scenario, the average ranks of the six models across ten benchmark datasets are shown in Table 4. Substituting these values into the Friedman formula gives

$$\sum_j R_j^2 = 78.48, \qquad \chi_F^2 = \frac{12\times 10}{6\times 7}(78.48 - 73.5) = 14.19,$$

and

$$F_F = \frac{9\times 14.19}{10\times 5 - 14.19} = 2.64.$$

With $k-1=5$ and $(k-1)(N-1)=45$ degrees of freedom, the critical values at $\alpha = 0.05$ are $\chi^2_{0.95,5} = 11.07$ and $F_{0.95,5,45} = 2.45$. Since $14.19 > 11.07$ (or equivalently $F_F = 2.64 > 2.45$), the null hypothesis is rejected, indicating a statistically significant difference among models under the 30% labeled data.

**Case 2: 50% Labeled Data.** For the 50% labeled scenario, the corresponding average ranks are shown in 5. The Friedman statistic is computed as

$$\sum_j R_j^2 = 79.72, \qquad \chi_F^2 = \frac{12\times 10}{6\times 7}(79.72 - 73.5) = 17.78,$$

and

$$F_F = \frac{9\times 17.78}{10\times 5 - 17.78} = 3.06.$$

Given the same critical values ($\chi^2_{0.95,5} = 11.07$ and $F_{0.95,5,45} = 2.45$), we again have $17.78 > 11.07$ (or $F_F = 3.06 > 2.45$). Thus, significant performance differences exist among the models under the 50% labeled data.

**Post-hoc Nemenyi Test.** To further analyze pairwise differences, the Nemenyi test was applied, where the critical difference (CD) is defined as

$$\mathrm{CD} = q_\alpha\sqrt{\frac{k(k+1)}{6N}}, \tag{4.42}$$

with $q_{0.05} = 2.85$ for $k = 6$ algorithms. For $N = 10$, the CD is

$$\mathrm{CD} = 2.85\sqrt{\frac{6\times 7}{6\times 10}} = 2.384.$$

Any pair of algorithms whose average-rank difference is smaller than $2.384$ is considered statistically similar at $\alpha = 0.05$. In our experiments, all pairwise rank differences involving MvLapPTSVM fell within this range, demonstrating that MvLapPTSVM performs

competitively with other models while maintaining the lowest average rank according to the Nemenyi criterion.

4.2. **Discussion.** The experimental results indicate that the proposed MvLapPTSVM model achieves competitive and stable classification performance across multiple benchmark datasets under both 30% and 50% labeled-data settings. The effectiveness of the framework can be attributed to the integration of multiview learning, Laplacian manifold regularization, and the pinball loss function, which collectively enhance robustness and generalization in semi-supervised classification tasks. The proposed model performs particularly well on datasets such as *Ionosphere*, *Diabetes*, *Monk-2*, and *Spectfheart*, indicating that the Laplacian regularization effectively captures the intrinsic manifold structure and utilizes unlabeled data to improve classification stability. In addition, the pinball loss function reduces sensitivity to noisy samples and outliers, resulting in more consistent performance across different folds.

The multiview framework further improves classification capability by integrating complementary information from the original and PCA-transformed feature representations. The co-regularization mechanism encourages consistency between views while preserving view-specific characteristics, leading to improved generalization compared with the single-view LapPTSVM model. Overall, the experimental findings confirm that MvLapPTSVM is an effective framework for semi-supervised multiview classification, particularly in scenarios with limited labeled data.

## 5. Conclusions

This study proposed MvLapPTSVM, a multi-view learning extension of LapPTSVM, designed to enhance classification performance by integrating multiple data views. Experimental results indicate that MvLapPTSVM performs particularly well on datasets where multi-view characteristics align with the underlying data structure. However, model complexity and parameter sensitivity remain important considerations for practical implementation. Therefore, careful parameter tuning and computational cost analysis are essential to fully realize the advantages of the proposed method in real-world applications.

## Acknowledgments

The authors would like to thank the referees for their careful reading and valuable suggestions. The authors also gratefully acknowledge the Faculty of Science at Sriracha, Kasetsart University. Second author was partially supported by Frontier Research and Innovation Cluster Fund, Naresuan University; Grant number R2569C008.

## References

[1] C. Cortes and V. Vapnik, Support-vector networks, Mach. Learn., vol. 20, no. 3, pp. 273–297, 1995.

[2] Kumar, M. A.; Gopal, M. Least squares twin support vector machines for pattern classification. *Expert Syst. Appl.* **36** (2009), no. 4, 7535–7543.

[3] Mei, B.; Xu, Y. Multi-task least squares twin support vector machine for classification. *Neurocomputing* **338** (2019), 26–33.

[4] Jayadeva; Khemchandani, R.; Chandra, S. Twin support vector machines for pattern classification. *IEEE Trans. Pattern Anal. Mach. Intell.* **29** (2007), no. 5, 905–910.

[5] Rastogi, R.; Sharma, S.; Chandra, S. Robust parametric twin support vector machine for pattern classification. *Neural Process. Lett.* **47** (2018), no. 1, 293–323.

[6] Tanveer, M.; Rajani, T.; Rastogi, R.; Shao, Y.-H.; Ganaie, M. A. Comprehensive review on twin support vector machines. *Ann. Oper. Res.* (2022), 1–46.

[7] Xie, X.; Sun, F.; Qian, J.; Guo, L.; Zhang, R.; Ye, X.; Wang, Z. Laplacian $L_p$ norm least squares twin support vector machine. *Pattern Recognit.* **136** (2023), 109192.

[8] Li, Y.; Sun, H. Safe sample screening for robust twin support vector machine. *Appl. Intell.* (2023), 1–17.
[9] Si, Q.; Yang, Z.; Ye, J. Symmetric LINEX loss twin support vector machine for robust classification and its fast iterative algorithm. *Neural Netw.* **168** (2023), 143–160.
[10] Gupta, U.; Gupta, D. Least squares structural twin bounded support vector machine on class scatter. *Appl. Intell.* **53** (2023), no. 12, 15321–15351.
[11] Rezvani, S.; Wang, X.; Pourpanah, F. Intuitionistic fuzzy twin support vector machines. *IEEE Trans. Fuzzy Syst.* **27** (2019), no. 11, 2140–2151.
[12] Xu, Y.; Yang, Z.; Pan, X. A novel twin support-vector machine with pinball loss. *IEEE Trans. Neural Netw. Learn. Syst.* **28** (2016), no. 2, 359–370.
[13] Demšar, J. Statistical comparisons of classifiers over multiple data sets. *J. Mach. Learn. Res.* **7** (2006), 1–30.
[14] Huang, X.; Shi, L.; Suykens, J. A. K. Support vector machine classifier with pinball loss. *IEEE Trans. Pattern Anal. Mach. Intell.* **36** (2013), no. 5, 984–997.
[15] García, S.; Fernández, A.; Luengo, J.; Herrera, F. Advanced nonparametric tests for multiple comparisons in the design of experiments in computational intelligence and data mining: Experimental analysis of power. *Inform. Sci.* **180** (2010), no. 10, 2044–2064.
[16] Tanveer, M.; Sharma, A.; Suganthan, P. N. General twin support vector machine with pinball loss function. *Inform. Sci.* **494** (2019), 311–327.
[17] Tanveer, M.; Tiwari, A.; Choudhary, R.; Jalan, S. Sparse pinball twin support vector machines. *Appl. Soft Comput.* **78** (2019), 164–175.
[18] Rastogi, R.; Pal, A.; Chandra, S. Generalized pinball loss SVMs. *Neurocomputing* **322** (2018), 151–165.
[19] Panup, W.; Ratipapongton, W.; Wangkeeree, R. A novel twin support vector machine with generalized pinball loss function for pattern classification. *Symmetry* **14** (2022), no. 2, 289.
[20] Alloghani, M.; Al-Jumeily, D.; Mustafina, J.; Hussain, A.; Aljaaf, A. J. A systematic review on supervised and unsupervised machine learning algorithms for data science. In: *Supervised and unsupervised learning for data science*, 3–21. Springer, 2020.
[21] Reddy, Y. C. A. P.; Viswanath, P.; Reddy, B. E. Semi-supervised learning: A brief review. *Int. J. Eng. Technol.* **7** (2018), no. 1.8, 81.
[22] Qi, Z.; Tian, Y.; Shi, Y. Laplacian twin support vector machine for semi-supervised classification. *Neural Netw.* **35** (2012), 46–53.
[23] Chen, W.-J.; Shao, Y.-H.; Deng, N.-Y.; Feng, Z.-L. Laplacian least squares twin support vector machine for semi-supervised classification. *Neurocomputing* **145** (2014), 465–476.
[24] Damminsed, V.; Panup, W.; Wangkeeree, R. Laplacian twin support vector machine with pinball loss for semi-supervised classification. *IEEE Access* **11** (2023), 31399–31416.
[25] Tanveer, M.; Tiwari, A.; Choudhary, R.; Ganaie, M. A. Large-scale pinball twin support vector machines. *Mach. Learn.* **111** (2022), no. 10, 3525–3548.
[26] Quadir, A.; Tanveer, M. Multiview learning with twin parametric margin SVM. *Neural Netw.* **180** (2024), 106598.
[27] Tanveer, M.; Ganaie, M. A.; Bhattacharjee, A.; Lin, C.-T. Intuitionistic fuzzy weighted least squares twin SVMs. *IEEE Trans. Cybern.* **53** (2022), no. 7, 4400–4409.
[28] Chen, H.; Xie, X.; Li, D. Semi-supervised learning with Deep Laplacian Support Vector Machine. *Pattern Anal. Appl.* **28** (2025), no. 1, 14.
[29] Dheeru Dua and Casey Graff. UCI machine learning repository. Available: http://archive.ics.uci.edu/ml, 2017.
[30] Luo, Y.; Tao, D.; Xu, C.; Li, D.; Xu, C. Vector-valued multi-view semi-supervised learning for multi-label image classification. In: *Proc. AAAI Conf. Artif. Intell.* **27** (2013), no. 1, 647–653.
[31] Xie, X.; Sun, S. Multi-view Laplacian twin support vector machines. *Appl. Intell.* **41** (2014), no. 4, 1059–1068.

[1] Faculty of Science at Sriracha, Kasetsart University, Sriracha Campus, Chonburi 20230, Thailand
*Email address*: vipavee.d@ku.th

[2] Department of Mathematics, Faculty of Science, Naresuan University, Phitsanulok, 65000, Thailand
*Email address*: rabianw@nu.ac.th